Parasitic Infections

5

Bryan H. Schmitt

While this chapter details many of the most frequently encountered parasites in anatomic pathology, it is by no means an exhaustive treatment of the subject. Additionally, certain regions of the world may be endemic for parasites not frequently encountered in pathology practices of the United States. For the identification of these less frequently encountered organisms, many extensive medical parasitology texts are available. In addition, the CDC DPDx website (http://www.cdc.gov/DPDx) is an excellent resource as well as a provider of authoritative consulting services.

5.1 Helminth Infections

Helminths encompass the parasitic worms. They are typically large and visible to the naked eye, unlike most other infectious agents. As such, identification is often more easily accomplished by gross observation rather than by histologic section. If a specimen is identifiable as a worm when received in the gross room, it is advisable to forward the organism to the microbiology lab as the first line for identification, with follow-up sections as needed. Parasitic helminths, particularly those that inhabit the gastrointestinal tract, also have characteristic eggs that may be expressed from the organism and identified in microbiology. On histopathologic examination, eggs are frequently present within or around the worms and may also provide valuable information regarding the identity of the organism; therefore many of the common egg morphologies are also discussed in this chapter.

B.H. Schmitt (✉)
Department of Pathology and Laboratory Medicine, Indiana University School of Medicine, Indianapolis, IN, USA
e-mail: bhschmit@iupui.edu

B.H. Schmitt (ed.), *Atlas of Infectious Disease Pathology*,
Atlas of Anatomic Pathology, DOI 10.1007/978-3-319-54702-2_5

5.1.1 Cestode Infections

Cestodes are more commonly known as "tapeworms," generally having ribbon-like bodies consisting of a scolex, or head, of the organism, a neck, and multiple proglottids containing reproductive structures and eggs. The larger members, such as *Taenia* and *Diphyllobothrium* species, may reach several meters or more in length, consisting almost entirely of a chain of proglottids. Since the proglottids are typically numerous and designed to break off in segments, they are much more likely to be encountered in anatomic pathology rather than the comparatively minute scolex and head structures (Figs. 5.1, 5.2, 5.3, 5.4, 5.5, 5.6, 5.7, 5.8, 5.9, 5.10, 5.11, 5.12, 5.13, 5.14, 5.15, 5.16, 5.17, 5.18, 5.19, 5.20, 5.21 and 5.22).

Fig. 5.1 Low magnification of a proglottid of *T. saginata*. Proper mounting of histopathologic specimens in order to demonstrate the uterine branching of *Taenia* species is difficult but was performed very well in this case owing to prior notification. Note that greater than 13 uterine branches (counted off one side only) are seen. *T. solium,* the second most frequently encountered *Taenia* species and cause of cysticercosis, has less than 13 branches. It should also be mentioned that *T. asiatica* will demonstrate greater than 13 uterine branches, similar to *T. saginata*. Infection with *T. asiatica* appears to be geographically restricted to parts of Asia as the name would suggest, and it is currently unclear whether *T. asiatica* is capable of causing cysticercosis. Hematoxylin and eosin (H&E), 20× magnification (Image courtesy of Jean Siders)

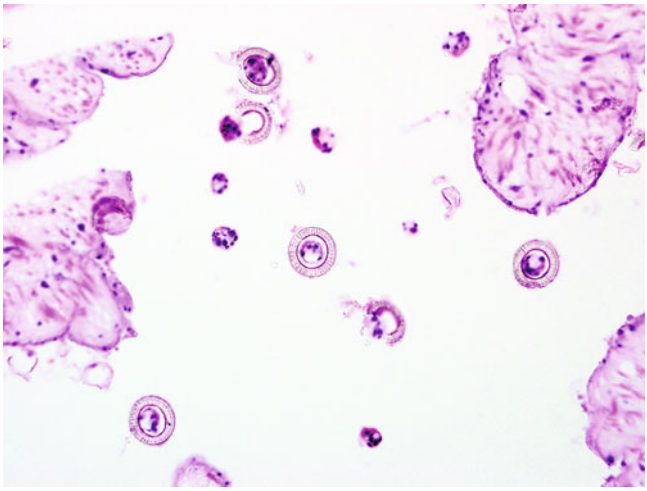

Fig. 5.2 Classic appearance of the eggs of *Taenia* species are seen in this case within the uterine branches. Note the thick shell, which demonstrates characteristic radial striations appearing similar to tightly packed "spokes on a wheel." In mature eggs, refractile hooklets are often visible in the center of the egg. Since eggs of *Taenia* species are essentially indistinguishable, patient history or examination of the uterine branches if possible is essential to making the correct identification. H&E, 400× magnification

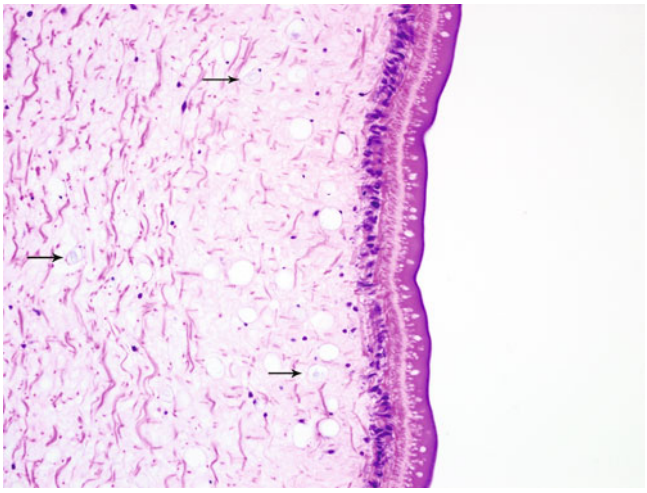

Fig. 5.3 An image of the proglottid wall. Note the thick cuticle, which is a common feature of many helminths. Characteristic for cestodes, however, are the many calcareous corpuscles (*arrows*), which are layered deposits of calcium carbonate often appearing as clear staining or purple laminated bodies within the walls of cestodes or within cestode-associated cyst fluid. H&E, 400× magnification

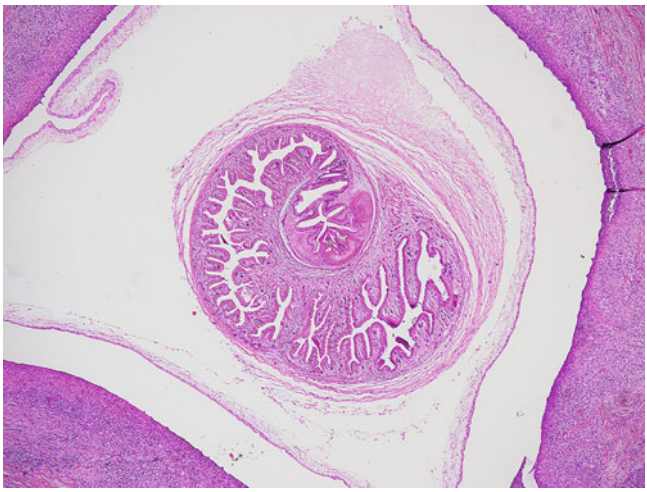

Fig. 5.4 Cysticercosis caused by infection with the larval stage of *T. solium* can manifest in nearly any organ system. However, infection of the central nervous system or "neurocysticercosis" is particularly devastating, leading to seizures and other neural disorders. The eggs of *T. solium* are autoinfectious to humans and may also pose a risk to contacts, whereas ingestion of *T. saginata* eggs does not lead to the development of cysticercosis. Differentiation of the two species may therefore be important for the purpose of treatment of patient contacts. Seen here is the typical appearance of a live *T. solium* cyst demonstrating the invaginated neck and head region of the protoscolex. Brain biopsy. H&E, 40× magnification

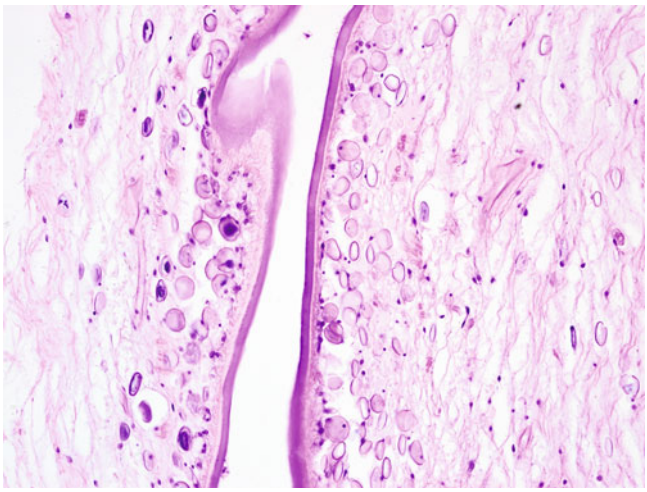

Fig. 5.5 Higher magnification of the cysticercus demonstrates numerous purple staining, calcareous corpuscles that are characteristic for cestode tissue. This finding may be very helpful in the identification of tapeworm parts, when scant tissue is present or if the plane of section does not demonstrate other characteristic structures. H&E, 400× magnification

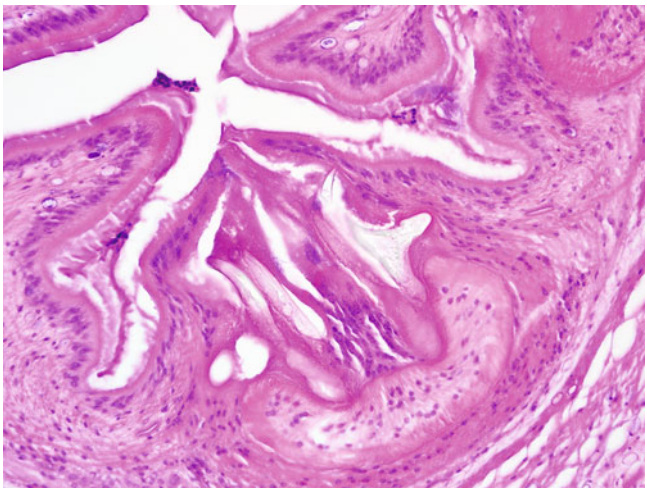

Fig. 5.6 A section of the tissue from the case seen in Fig. 5.4 demonstrating rows of refractile appearing hooklets. Adjustment into differing planes of focus often highlights these structures. H&E, 1000× magnification

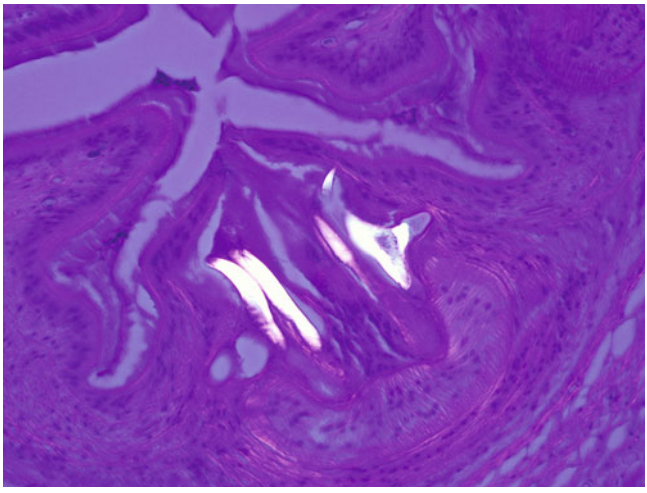

Fig. 5.7 Hooklets of cestodes in general are often birefringent and appear bright under polarized light. H&E, 1000× magnification

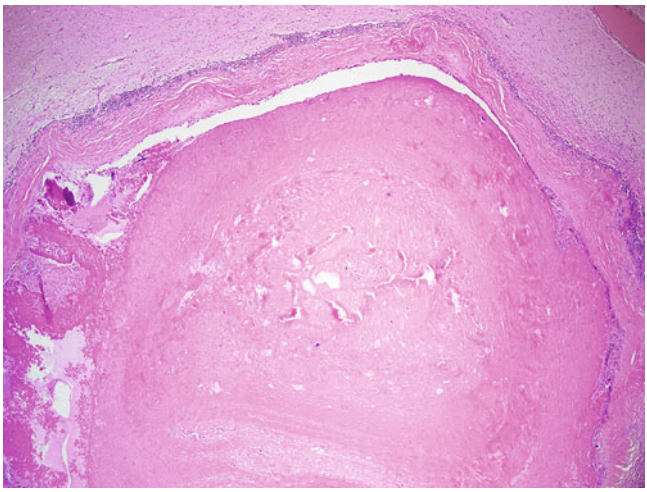

Fig. 5.8 A "dead" cyst in a case of neurocysticercosis identified at autopsy from a patient who had developed seizures, a common complication of neurocysticercosis. The inflammatory host response in reaction to dying cysticerci is significantly greater than when they are live, initially recruiting a dense acute inflammatory infiltrate and eosinophils and later a chronic granulomatous response. Eventually the cyst develops a thick fibrotic wall that may also demonstrate significant calcification. H&E, 40× magnification

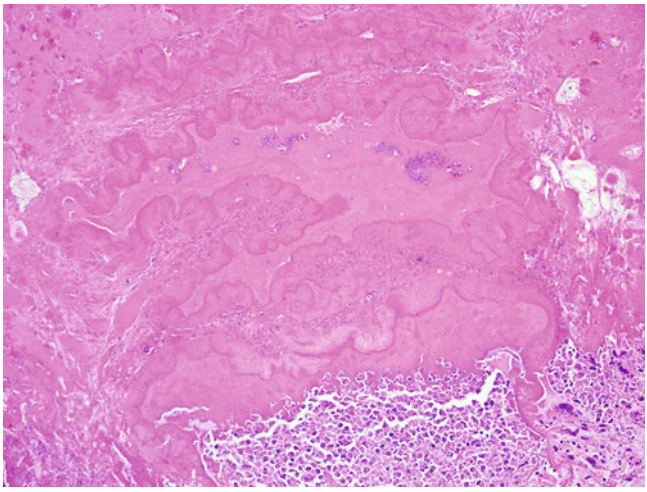

Fig. 5.9 "Ghosted-out" folds or invaginations can still be identified in this specimen. The appearance is similar to that seen in coagulative necrosis. H&E, 200× magnification

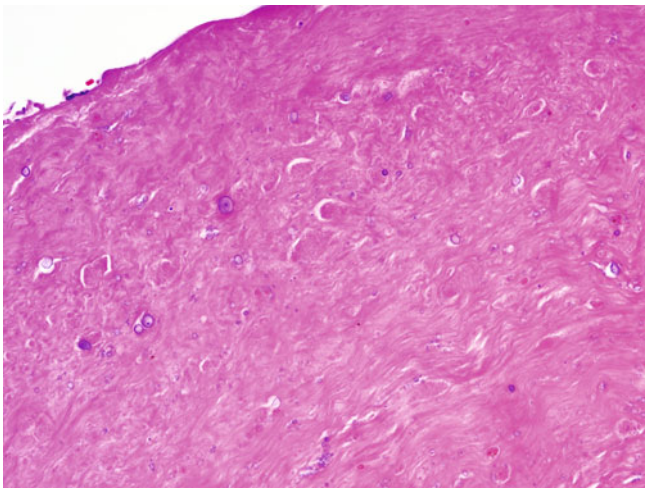

Fig. 5.10 Calcareous corpuscles frequently remain behind in the necrotic cysticercus and may be the only means of identification as a cestode infection. H&E, 400× magnification

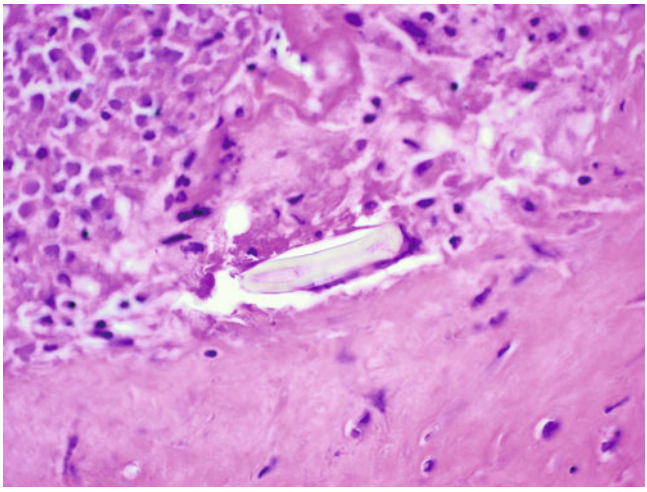

Fig. 5.11 Higher magnification of the case from Figs. 5.8, 5.9 and 5.10. In addition to calcareous corpuscles, refractile hooklets may occasionally be found within the degenerated material. H&E, 600× magnification

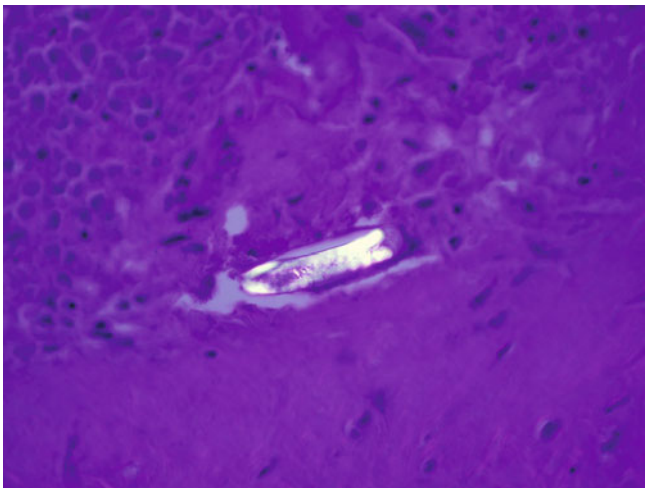

Fig. 5.12 The hooklet demonstrated in Fig. 5.11 under polarized light. This quality may help ascertain if the object is indeed a hooklet or if it is other mineralized material or debris. H&E, 600× magnification

Fig. 5.13 Of the large tapeworms that routinely infect humans, *Diphyllobothrium latum* along with *Taenia* species are likely the most frequently encountered, depending on geographic location. They can be distinguished by the shape of the mature proglottids being broader than long; hence the term "broad fish tapeworm." Note that the uterus has a characteristic "rosette" pattern differing from the branching pattern of *Taenia* species. Carmine stain, 20× magnification

Fig. 5.14 The eggs of *D. latum* are also significantly different in appearance from those of *Taenia* species. The eggs are larger and have a "hatch" at one end (the operculum, denoted by an *arrow*) as well as a subtle abopercular knob or thickening at the opposite end. The eggs may be seen in proglottids but can also be encountered near the luminal surface of lower gastrointestnal tract specimens. Wet mount, 400× magnification (Image courtesy of Dr. Ryan Relich)

Fig. 5.15 *Dipylidium caninum* most commonly infects dogs and cats but can be transferred to humans through the ingestion of fleas harboring the cysticercoid stage. The proglottids are small, resembling rice grains, and they are often actively moving when freshly passed. Observation of "egg packets" within a sectioned proglottid or gastrointestinal tract specimen is characteristic. H&E, 100× magnification

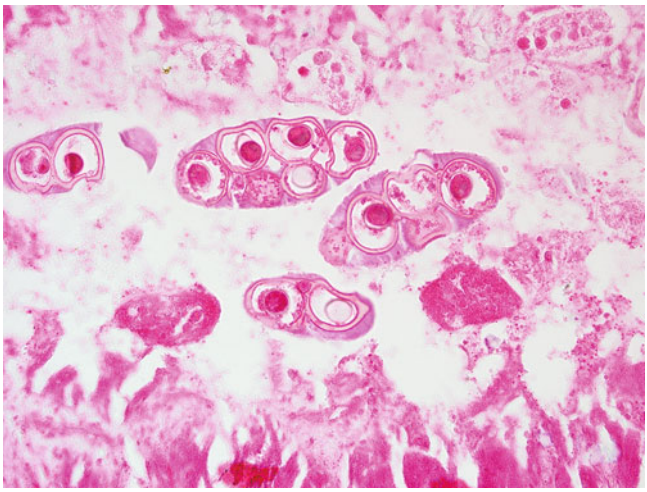

Fig. 5.16 Higher magnification demonstrating eggs clustered together in "packets" surrounded by a thin membrane. More mature eggs may demonstrate sets of internal hooklets. H&E, 400× magnification

Fig. 5.17 Adult *Echinococcus granulosus*. These cestodes are significantly smaller than the previously discussed species. Adults measure up to 6 mm and demonstrate three proglottids in varying stages of maturation. As canines are the definitive host, adults are not typically encountered as anatomic pathology specimens. Humans act as an intermediate host in which hydatid cyst forms are seen. Whole mount, carmine stain, 40× magnification

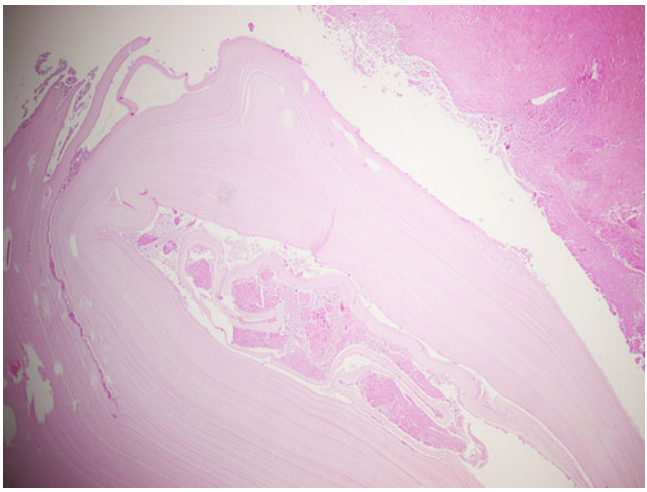

Fig. 5.18 Degenerated hydatid cyst of the liver caused by infection of *E. granulosus*. Note that *E. granulosus* typically produces a thick, unilocular cyst wall that has a prominent laminated appearance. Prior rupture of the cysts resulting from trauma or medical procedures may cause the formation of additional, usually adjacent cysts; however, the laminated appearance should be preserved. H&E, 40× magnification

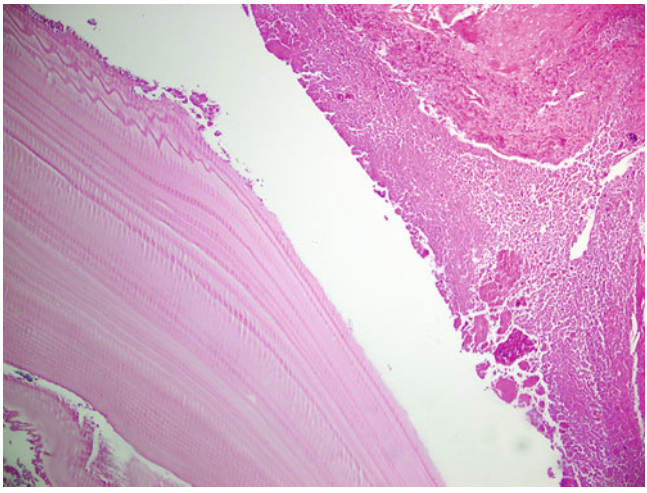

Fig. 5.19 Higher magnification image demonstrating prominent lamination of the cyst wall. H&E, 100× magnification

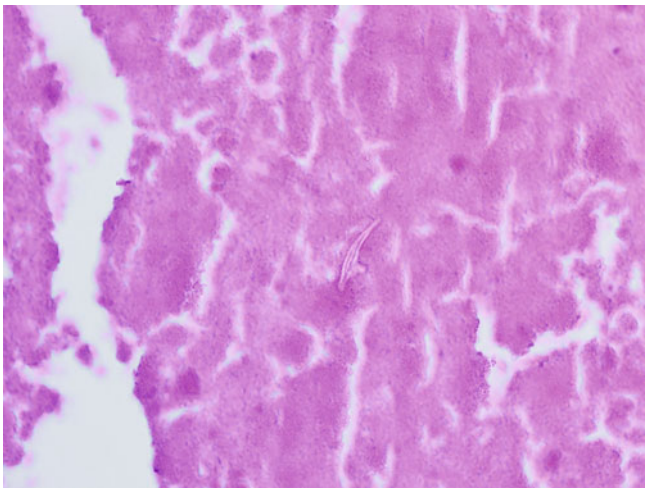

Fig. 5.20 In this particular case, rare refractile hooklets could be found within the degenerating cellular material. H&E, 1000× magnification

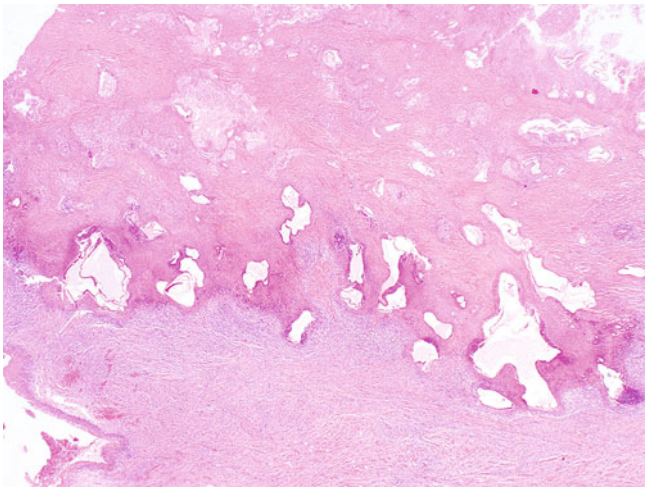

Fig. 5.21 An example of *Echinococcus multilocularis* infection in liver tissue. *E. multilocularis* infections can be differentiated from those of *E. granulosus* in that there are usually multiple thin-walled cysts present that will invade through tissue and may even demonstrate dissemination. The cysts are also often multilocular, as the name would suggest. H&E, 20× magnification (Image courtesy of Dr. Bobbi Pritt)

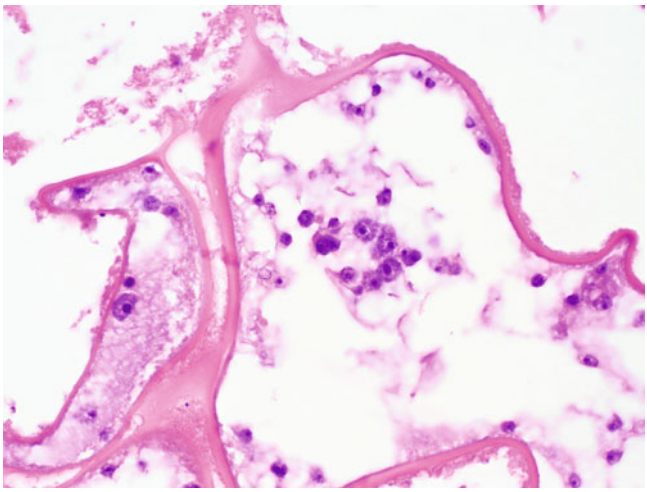

Fig. 5.22 Higher magnification image demonstrating multilocular cysts of *E. multilocularis*. The walls are thinner than those of *E. granulosus,* and while laminations may be present, they are not nearly as prominent. Protoscolices are not usually indentified. H&E, 1000× magnification (Image courtesy of Dr. Bobbi Pritt)

5.1.2 Trematode Infections

The trematodes are a group of parasitic flatworms, more commonly known as flukes. The most well known of this group are the schistosomes, the adults of which inhabit the mesenteric or urinary plexus, depending on species. As these areas are infrequently surgically sampled, schistosome infections are most commonly identified by detection of their eggs in stool, urine, or on biopsy of the lower gastrointestinal tract or urinary bladder. Other trematodes such as *Clonorchis*, *Opisthorchis*, or *Fasciola* species have a predilection for the biliary system, while *Paragonimus* species are most frequently found within pulmonary tissue (Figs. 5.23, 5.24, 5.25, 5.26, 5.27, 5.28, 5.29, 5.30, 5.31, 5.32, 5.33, 5.34, 5.35, 5.36, 5.37, 5.38, 5.39, 5.40 and 5.41).

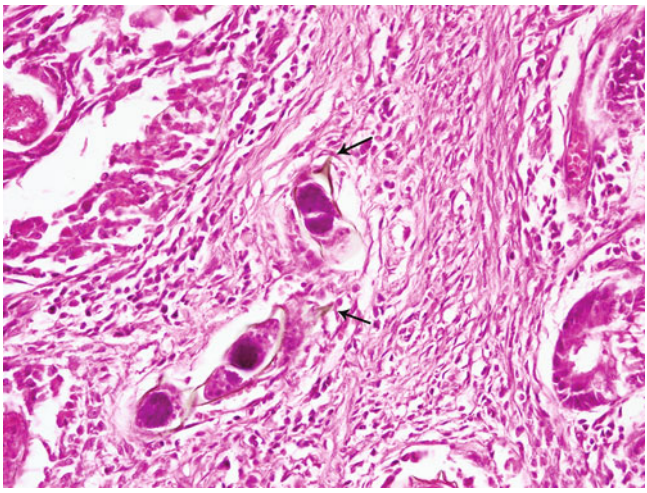

Fig. 5.23 Adult schistosomes are rarely identified in anatomic pathology tissue. Instead, their characteristic eggs are seen. The eggs of *Schistosoma mansoni*, the most well-known of the species, are usually seen in the mucosa of the lower gastrointestinal tract, often causing a polyp-like mass that is biopsied at routine colonoscopy. Shown here is the characteristic appearance of eggs of *S. mansoni,* which demonstrate a large lateral spine. The spines may be very difficult to identify on histopathologic examination because their appearance depends largely on the plane of section. While not seen here, significant calcification of the eggs, particularly in longstanding lesions, may be present. H&E, 400× magnification

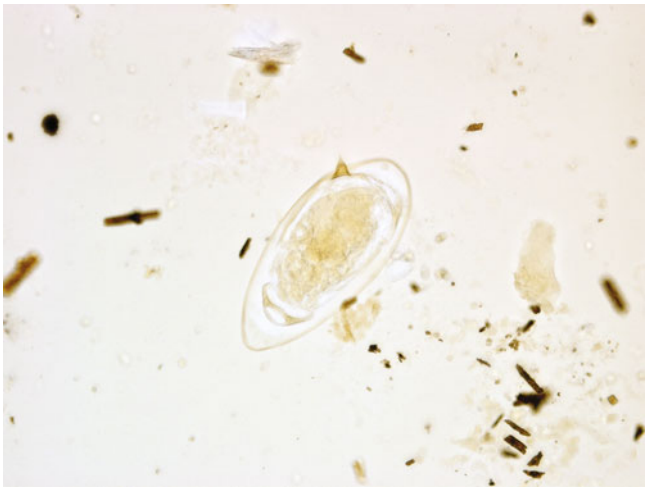

Fig. 5.24 *S. mansoni* egg from an iodine-stained stool microscopic examination demonstrating the classic appearance of the large lateral spine. 400× magnification

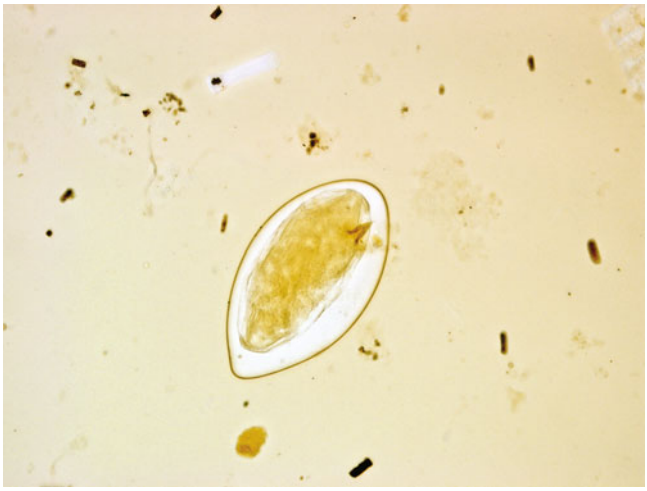

Fig. 5.25 A rotated *S. mansoni* egg from the same preparation. Here the spine is positioned toward the microscopist. A histologic section taken with an egg oriented in this manner likely would not demonstrate the characteristic lateral spine. 400× magnification

Fig. 5.26 An adult male *S. mansoni* fluke. Note the gynecophoral canal (*arrows*) in which the copulating female fluke resides. Carmine stain, whole mount, 40× magnification

Fig. 5.27 An adult female *S. mansoni* fluke. Unlike the typical "flatworm" appearance of most trematodes, female schistosomes are cylindrical. Carmine stain, whole mount, 40× magnification

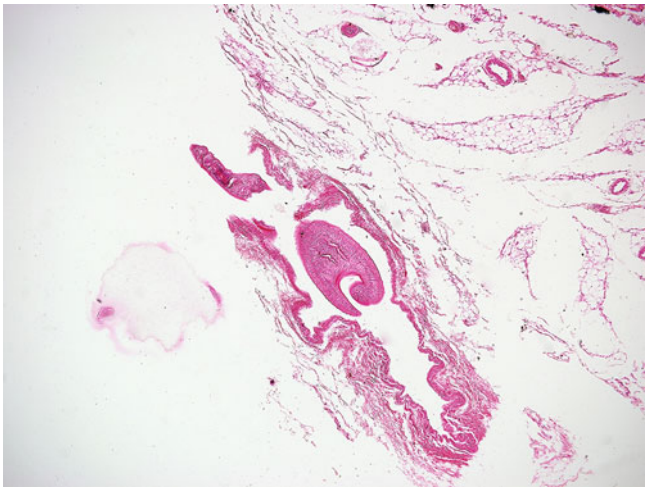

Fig. 5.28 Male *S. mansoni* within a mesenteric vein. Note that a whole mount, such as demonstrated in Fig. 5.26, might give the appearance of a cylindrical worm. Male shistosomes are in fact flat, curling their edges around copulating females. H&E, 40× magnification

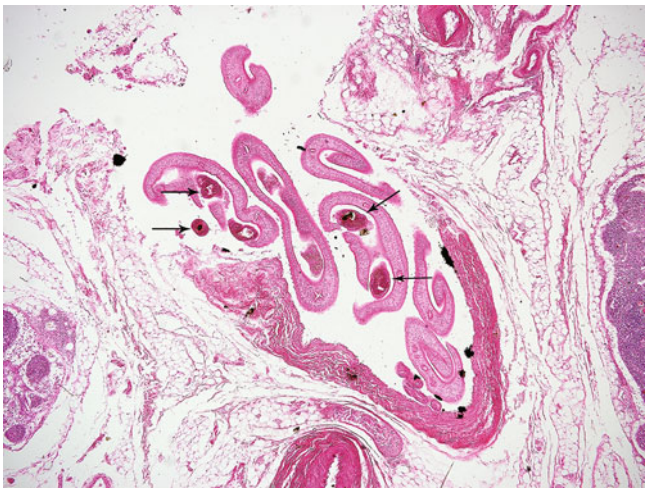

Fig. 5.29 Several copulating *S. mansoni* flukes within a mesenteric vein. Note cross-sections of female *S. mansoni* within the gynecophoral canals of males (*arrows*). H&E, 40× magnification

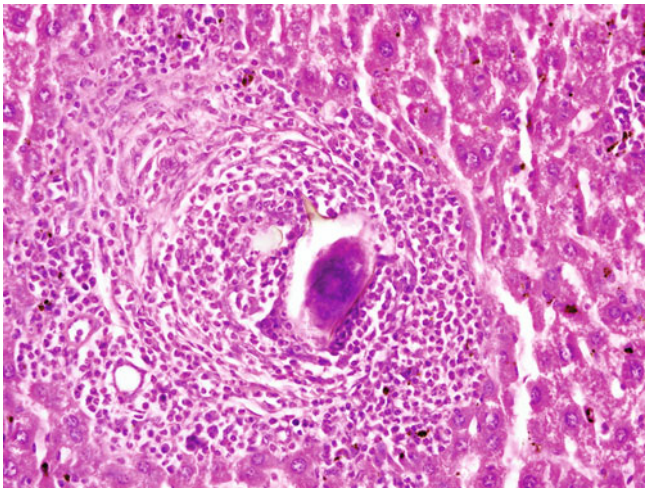

Fig. 5.30 While the colon is the primary site for migration of the eggs of *S. mansoni*, it is important to note that the eggs may be found in nearly any abdominal/pelvic location, with the liver, as seen here, another frequent destination. The prominent lateral spine in this image is diagnostic for *S. mansoni*. H&E, 400× magnification

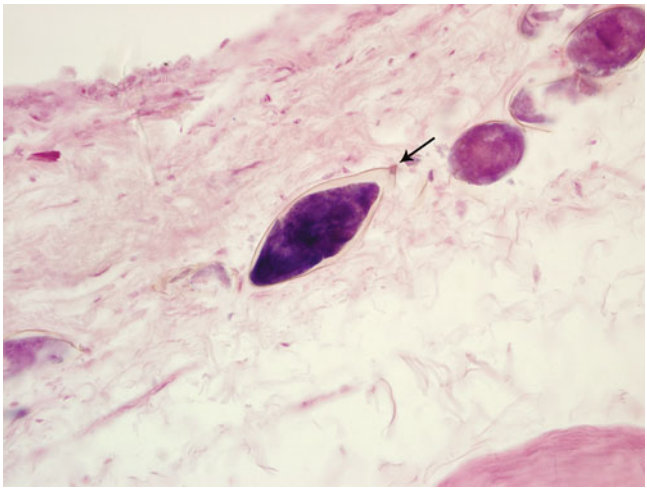

Fig. 5.31 In contrast to *S. mansoni*, *S. haematobium* is most frequently found within the urinary system, as the adults reside within the venous plexus surrounding the urinary bladder. Eggs of *S. haematobium* are more elongate than *S. mansoni* and feature a less prominent, terminal spine (*arrow*). H&E, 400× magnification

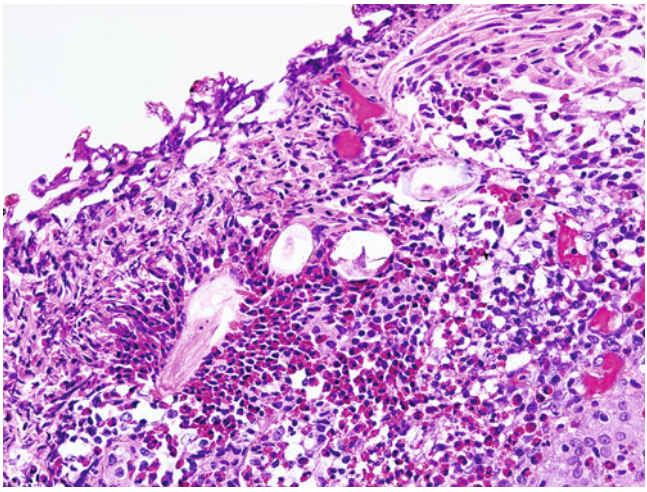

Fig. 5.32 *S. haematobium* eggs within the epithelium of the urinary bladder. The refractile shell of the eggs is readily apparent; however, the characteristic terminal spines are not. Note the elongate shape of the eggs and the location within the urinary bladder, which are good indicators of infection with *S. haematobium*. Note also a prominent eosinophilic inflammatory response, commonly seen with parasitic infections. H&E, 400× magnification

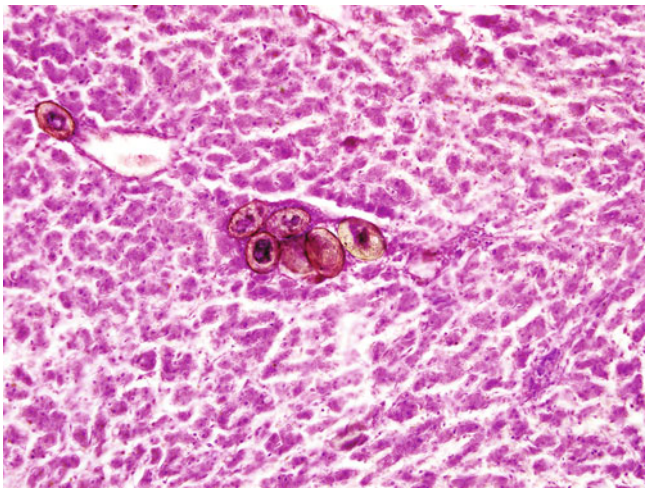

Fig. 5.33 *S. japonicum* seen in the liver. Like *S. mansoni*, the adult forms of *S. japonicum* usually reside in the mesenteric plexus and therefore, along with the colon, the liver is a frequent location where their eggs are identified. The eggs of *S. japonicum* are round to slightly oval and characteristically have a very small lateral spine, or nub, which is often unidentifiable. H&E, 200× magnification

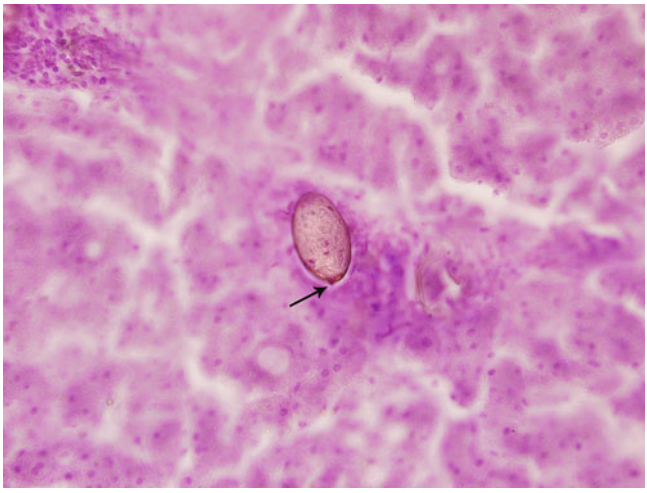

Fig. 5.34 The typical appearance of the small spine of *S. japonicum* eggs seen within a liver biopsy specimen (*arrow*). H&E, 400× magnification

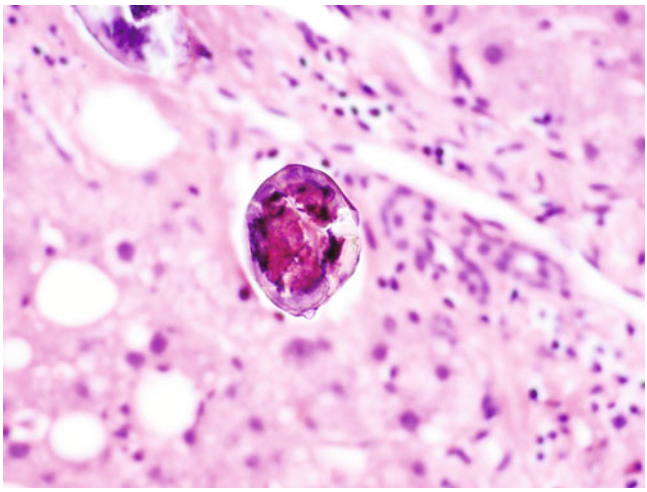

Fig. 5.35 A higher magnification image demonstrating the small lateral spine of *S. japonicum* in a partially calcified egg within the liver. Note that the liver tissue in the background is in a different plane of focus. Changing planes may be an important method to identify subtle features of infectious microorganisms. H&E, 600× magnification

Fig. 5.36 *Paragonimus* species, also known as "lung flukes," are large trematodes that typically infect the pulmonary system following ingestion of undercooked crustaceans. While most commonly found in Asia, where *P. westermani* is most common, infections in North America with *P. kellicotti* have been documented. After entering the lung following migration from the intestines, the worm exhibits a chronic and granulomatous inflammatory response which, over time, creates a fibrous "capsule" around the organism. H&E, 40× magnification

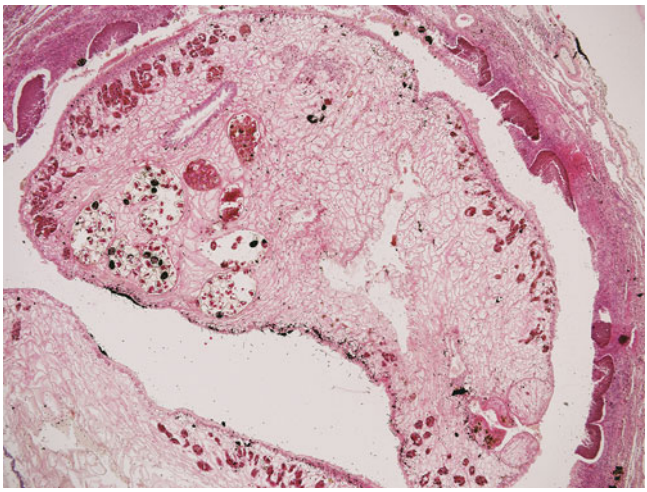

Fig. 5.37 Depending on where the fluke is sectioned, a significant perceived size variation may be noted, with the fluke appearing much larger if cut through the center. H&E, 40× magnification

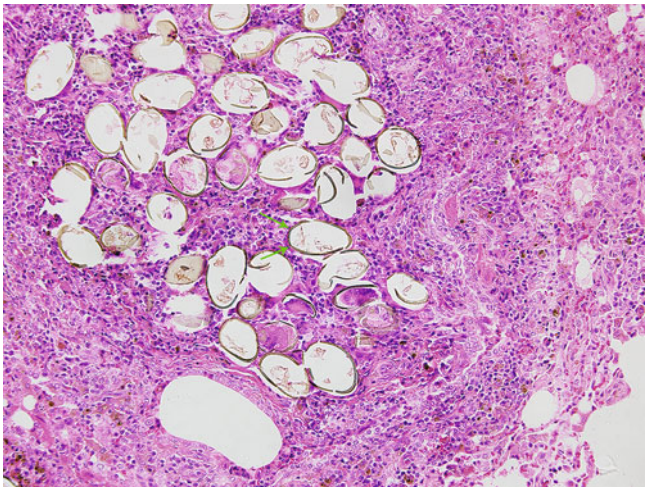

Fig. 5.38 The eggs of *Paragonimus* species are large, approximately 80–120 microns in length, and demonstrate a thick refractile shell. One end demonstrates a "shouldered" operculum having two tiny knobs on either side (*arrows*) and an opposite end that is slightly thickened. They may be identified within the fluke itself or scattered throughout the adjacent tissue, where they elicit a chronic and granulomatous inflammatory response. H&E, 200× magnification

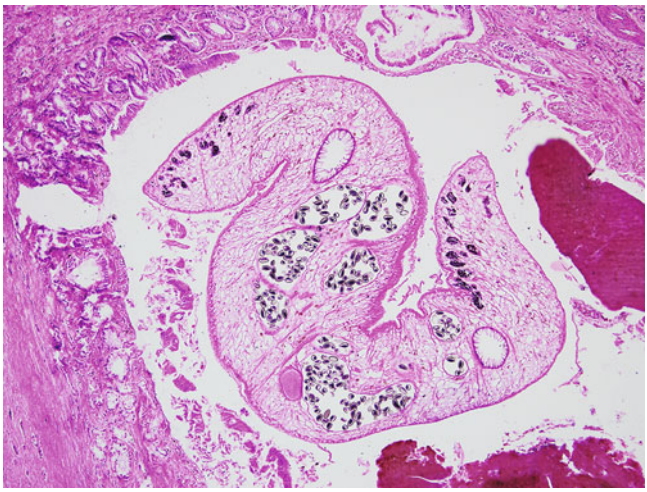

Fig. 5.39 *Clonorchis sinensis* within a bile duct. The liver flukes, *Clonorchis sinensis* and *Opisthorchis* species, are each small (10–15 mm in length) flukes that reside principally within the biliary duct system. Fibrosis and glandular hyperplasia are common features. *Fasciola* species reside within the hepatic biliary tree and are typically much larger (30–75 mm in length, depending on species). H&E, 100× magnification

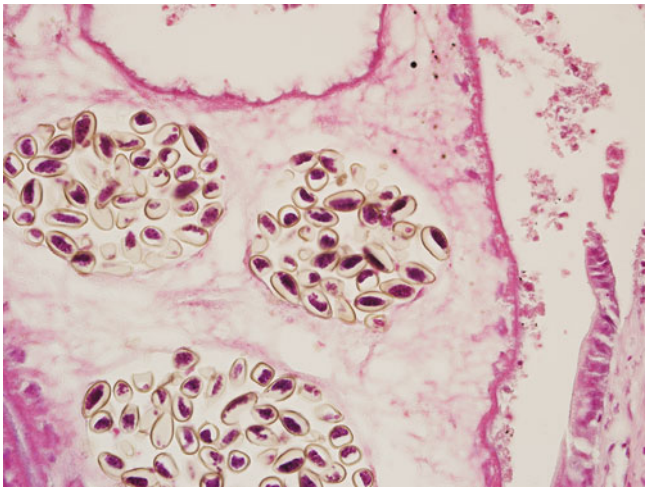

Fig. 5.40 At higher magnification, intrauterine clusters of eggs can be seen and may be helpful in making a diagnosis. H&E, 400× magnification

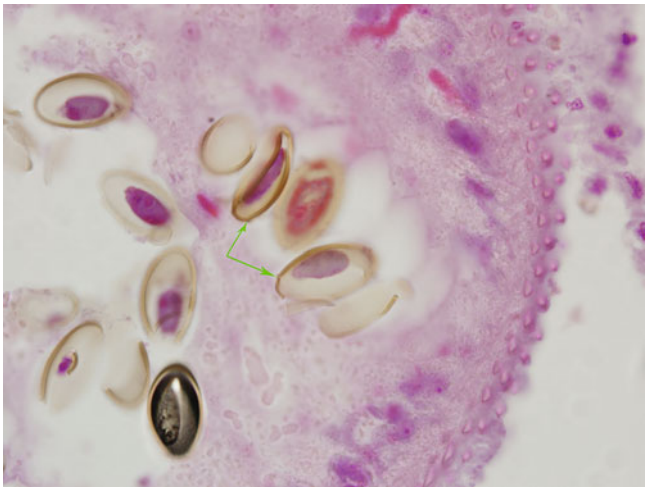

Fig. 5.41 The eggs of *Clonorchis* and *Opisthorchis* species are very similar in appearance and size (~25–35 μm long) and may be indistinguishable from each other. A "shouldered" (*arrows*) operculum is typically evident and a small abopercular knob may also be identified. The eggs are often described as being "urn-shaped."H&E, 1000× magnification

5.1.3 Nematode Infections

Nematodes are "roundworms" and are long and cylindrically shaped. They constitute the most common helminthic infections of humans, having a wide variety of members with humans as accidental, dead end, or definitive hosts, depending on the species. As such, they are associated with a wide variety of disease presentations (Figs. 5.42, 5.43, 5.44, 5.45, 5.46, 5.47, 5.48, 5.49, 5.50, 5.51, 5.52, 5.53, 5.54, 5.55, 5.56, 5.57, 5.58, 5.59, 5.60, 5.61, 5.62, 5.63, 5.64, 5.65, 5.66, 5.67 and 5.68).

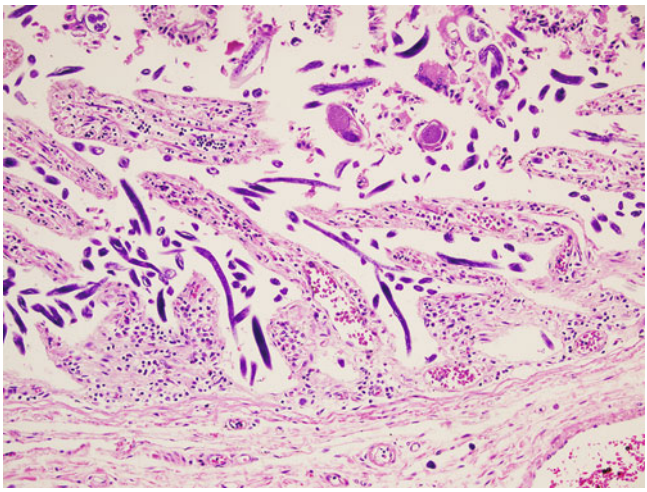

Fig. 5.42 *Strongyloides stercoralis,* also commonly known as "threadworm," most commonly causes an asymptomatic disease or mild gastrointestinal symptoms. Adult worms typically reside in the small intestine. However, the eggs they produce have the ability to hatch within the large intestine, producing rhabditiform larvae that may be excreted in the stool or mature into filariform larvae, which in turn migrate through the intestinal wall, through the bloodstream to the lungs, eventually returning to the small intestine where they can mature into adults, perpetuating the cycle known as "autoinfection." As a result of autoinfection, *Strongyloides* may persist in the gastrointestinal tract for the lifetime of the patient. While they usually cause asymptomatic or mild disease, patients who become immunocompromised may experience life-threatening "hyperinfection syndrome" in which high worm burdens migrate out of the gastrointestinal tract and throughout the body. As a result of mass migration though the intestinal wall, the first clinical manifestation of this disease is often bacteremia with enteric organisms. Small intestine demonstrating sections of many *Strongyloides* worms in a patient with hyperinfection syndrome. H&E, 200× magnification

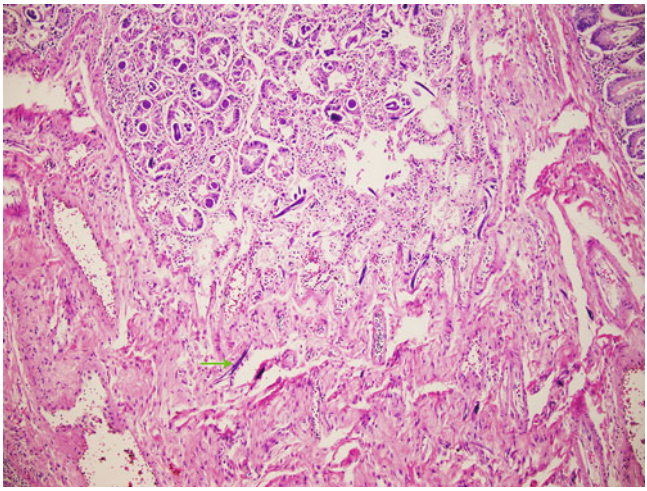

Fig. 5.43 In this image, several *Strongyloides* larvae (example at *arrow*) are seen migrating through the intestinal wall in a case of hyperinfection syndrome. H&E, 100× magnification

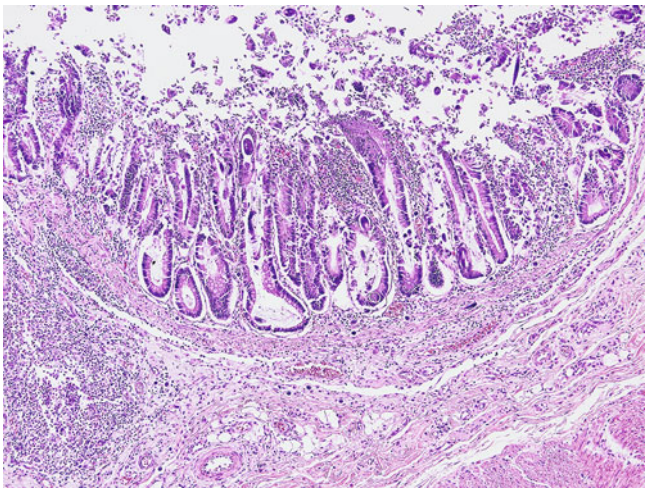

Fig. 5.44 Colon in a case of hyperinfection syndrome. Sections of migrating larvae are seen within the muscularis mucosa and submucosal layers. H&E, 100× magnification

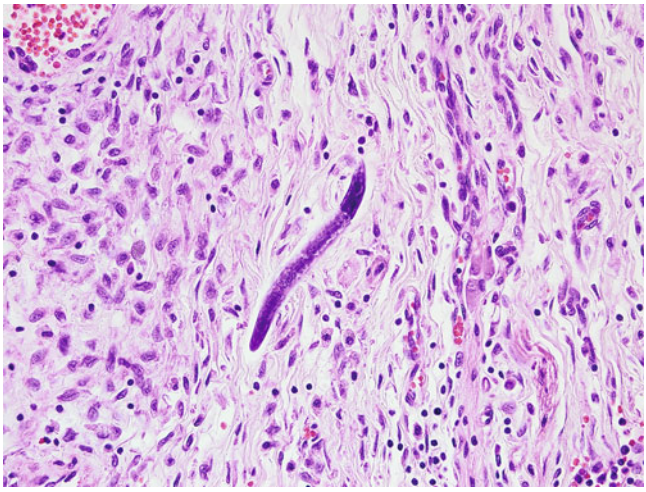

Fig. 5.45 High magnification image of migrating *Strongyloides* larva within the submucosa. H&E, 400× magnification

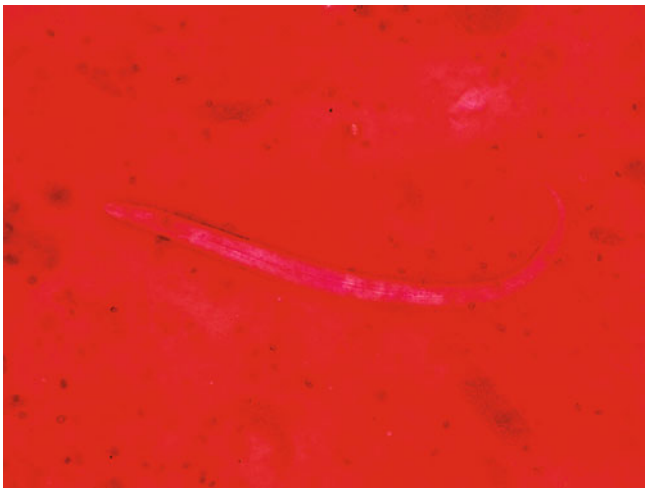

Fig. 5.46 Filariform larva of *S. stercoralis* from a bronchoalveolar lavage specimen. *S. stercoralis* migrating through the lungs may cause eosinophilic pneumonia (Loeffler syndrome). Gram stain, 400× magnification

Fig. 5.47 *Trichuris trichiura* is commonly known as "whipworm" because of its body shape with a thin, threadlike anterior portion and a larger posterior portion resembling a handle. The adults typically reside in the colon, where the anterior portion of their body burrows into the intestinal mucosa. While occasionally retrieved whole at colonoscopy, usually only fragments of the organism are seen in anatomic pathology specimens and may appear to be floating above the tissue surface, with the embedded head often not represented in sections. Here, sections of the non-embedded anterior portion of *T. trichuria* are seen in a colon biopsy. The esophagus is encircled by prominent unicellular glandular structures called stichocytes (*arrows*), with the series of these structures being known as a stichosome. H&E, 100× magnification

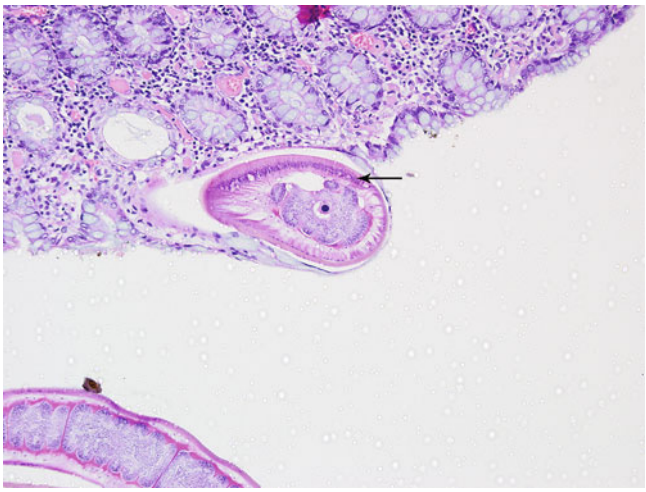

Fig. 5.48 A cross-section through a more anterior portion of the worm demonstrates the prominent nucleus of a stichocyte, along with a characteristic "bacillary band" (*arrow*), a basophilic staining row of columnar cells found in *Trichuris* and *Capillaria* species (not further discussed here). H&E, 200× magnification

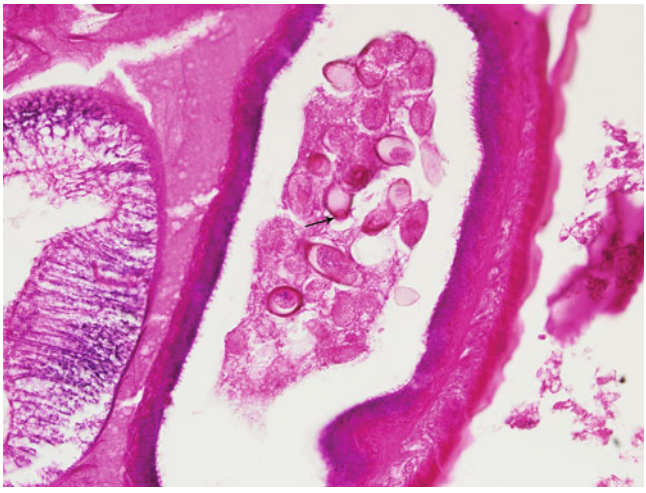

Fig. 5.49 Sections through the posterior end of gravid females may demonstrate characteristic oval eggs with "bipolar plugs" at each end. One of these plugs is demonstrated by the *arrow*. H&E, 400× magnification

Fig. 5.50 Egg of *T. trichuria* obtained from a stool wet mount. Note the characteristic, bipolar plugs. 400× magnification (Image courtesy of Dr. Ryan Relich)

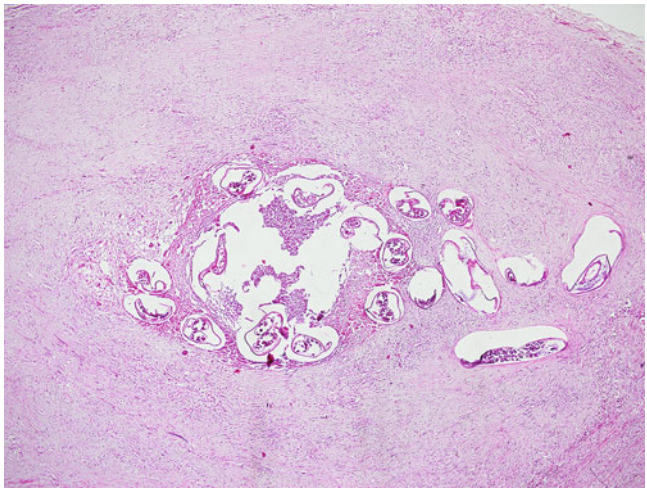

Fig. 5.51 Onchocerca volvulus, the causative agent of "river blindness," is transmitted by the bite of black flies of the genus *Simulium*. Adults typically reside in subcutaneous nodules along with the microfilarial forms. As such, microfilaria are not typically found in blood smears, which is the method of choice for the diagnosis of most other microfilarial infections. Instead, diagnosis is usually made by the examination of "skin snips" in which microfilaria can be found, or by histopathologic examination of subcutaneous nodules. Here is a subcutaneous nodule containing several adult worms. The adult worms induce a host fibroblastic reaction, leading to the formation of a fibrotic subcutaneous nodule. H&E, 40× magnification

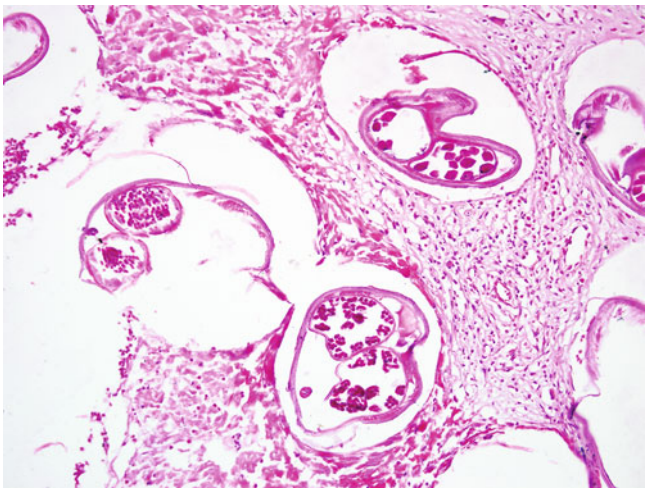

Fig. 5.52 Higher magnification image demonstrating cross-sections of microfilaria within the uteri of likely several adult females. H&E, 200× magnification

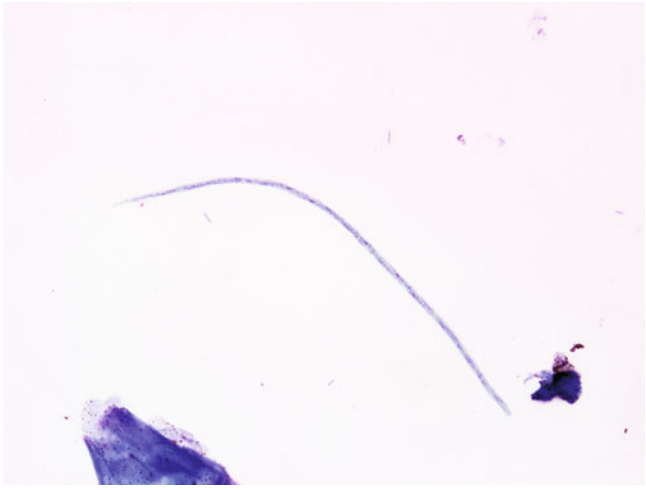

Fig. 5.53 A microfilaria of *O. volvulus*. Skin snips are typically placed in a physiologic solution such as saline, which causes the microfilaria to emerge, after which they can be examined microscopically. Giemsa stain, 500× magnification

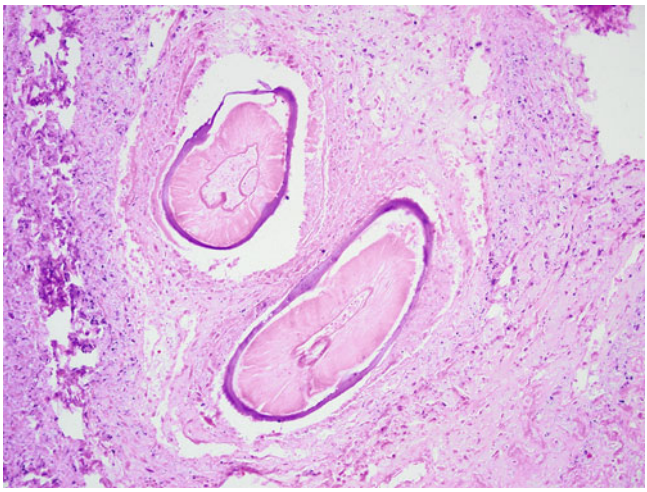

Fig. 5.54 *Dirofilaria* species typically infect carnivorous animals, particularly dogs and cats; however, humans are very rare hosts. While causing heartworm disease in most animals, in humans infection most often results in pulmonary infarcts caused by blockage of the pulmonary vessels. The species *D. repens* and *D. tenuis* have been implicated in subconjunctival lesions. A section of infarcted lung tissue caused by infection with *D. immitis*. Sections of the worm can be seen within the pulmonary vasculature. H&E, 200× magnification

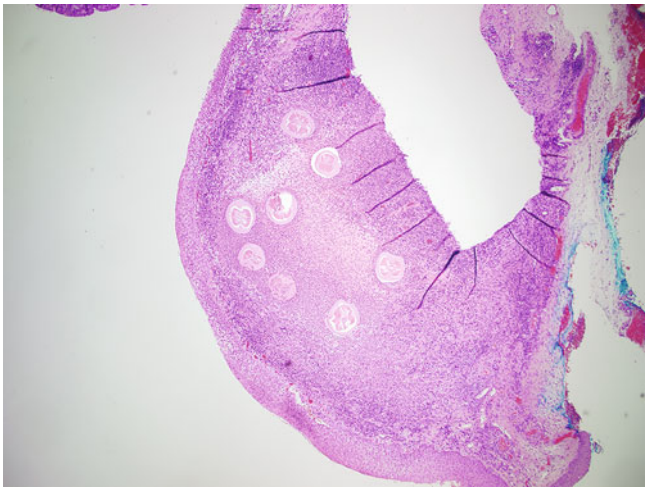

Fig. 5.55 Subconjunctival infection with *Dirofilaria* species. Note cross-sections of several worms surrounded by an intense inflammatory response. H&E, 40× magnification

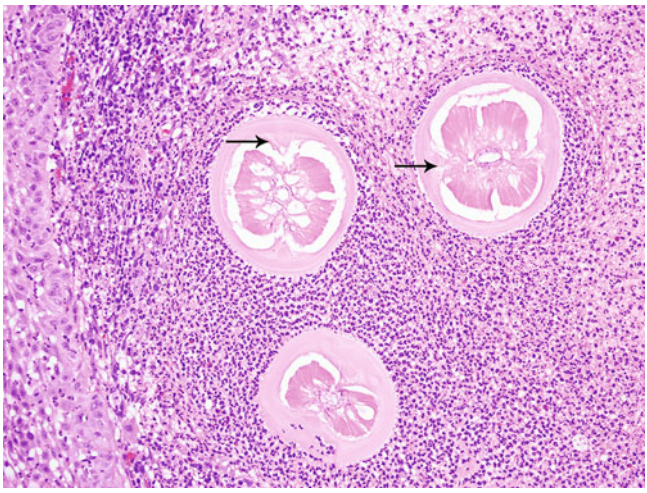

Fig. 5.56 Higher magnification image demonstrating prominent internal lateral ridges (*arrows*), a characteristic feature of this organism. Note also that within the primarily neutrophilic infiltrate, a few scattered eosinophils are seen, a common response to nematode infections. H&E, 200× magnification

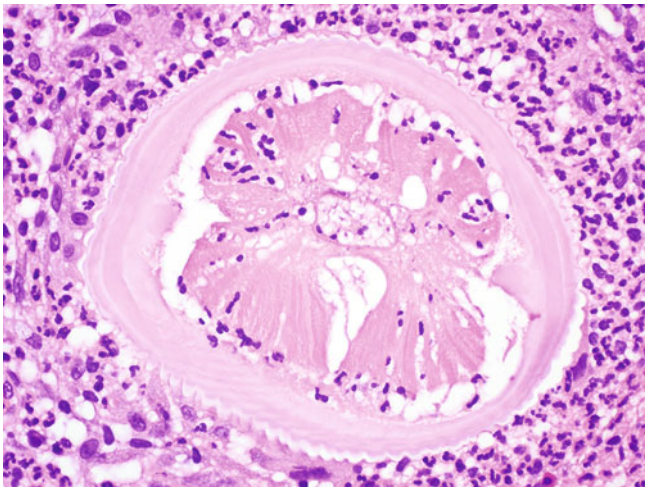

Fig. 5.57 High magnification image, again demonstrating prominent internal lateral ridges. In this particular example, neutrophils can be seen invading through the worms' internal musculature. Prominent ridging of the external cuticular surface can also be seen. H&E, 400× magnification

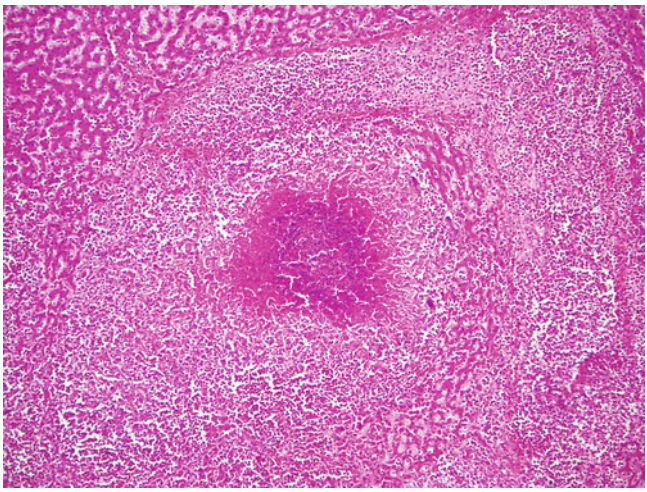

Fig. 5.58 Toxocariasis is caused by larval forms of nematodes of the *Toxocara* genus, most frequently *T. canis,* which primarily infects dogs and *T. felis,* which primarily infects cats. Humans become infected by ingestion of eggs, typically through contaminated soil. The eggs hatch in the intestine and the larvae migrate throughout the body, most typically the heart, brain, liver, lungs, and muscle (visceral larva migrans, VLM). However, they also may migrate to the eye. Visceral infections are usually accompanied by eosinophilia. As the worms are rarely identified in tissue, the mainstay of diagnosis relies on serology**.** A case of VLM involving the liver is shown. Classically migration of the organism causes the production of palisading granulomas containing eosinophils. The larvae themselves are not seen in this example. H&E, 100× magnification

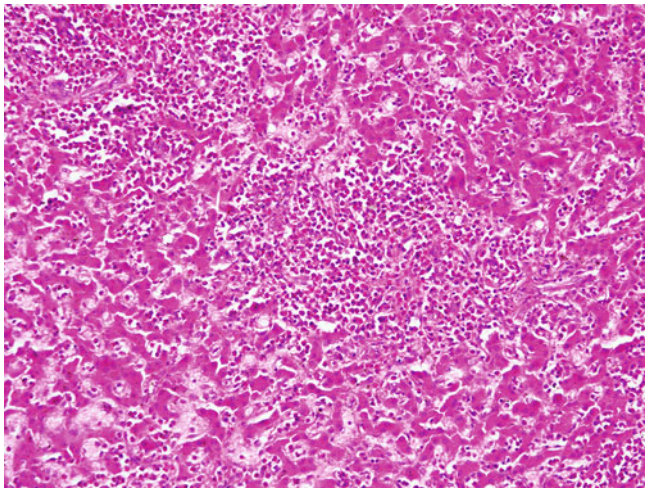

Fig. 5.59 Higher magnification image demonstrating a predominantly eosinophilic inflammatory response. H&E, 200× magnification

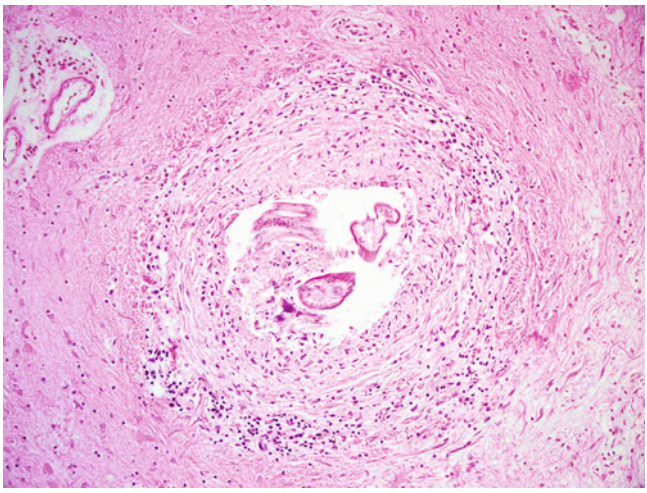

Fig. 5.60 *Baylisascaris procyonis* is the cause of baylisascariasis in humans. Primarily an intestinal nematode of raccoons and occasionally dogs, humans can come in contact with the eggs through environmental sources. Like toxocariasis, widespeard dissemination occurs, and both visceral and ocular larval migrans forms exist. However, the larval forms of *Baylisascaris* are larger, and do not readily die in human tissue and continue to mature. Because of this feature, infection of *Baylisascaris* tends to cause more severe disease. *Baylisascaris* migration also seems to prefer the central nervous system and ocular structures, which may result in permanent disability or death. *Baylisascaris* larvae in brain tissue. H&E, 200× magnification

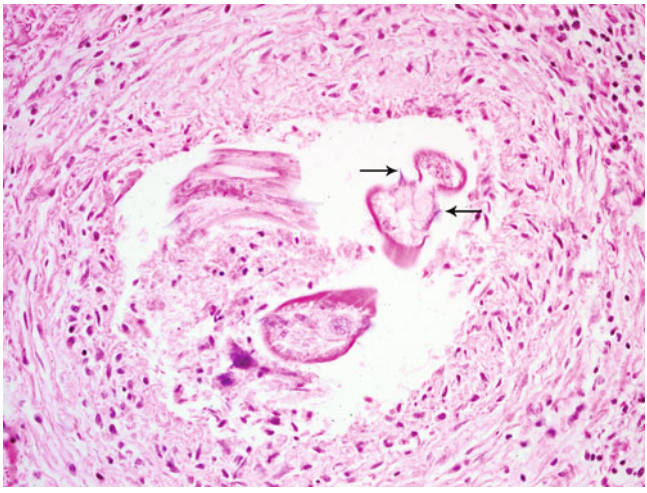

Fig. 5.61 Higher magnification image. Lateral alae or "wings" (*arrows*) are frequently identified in sections of the larvae of *Baylisascaris*. H&E, 400× magnification

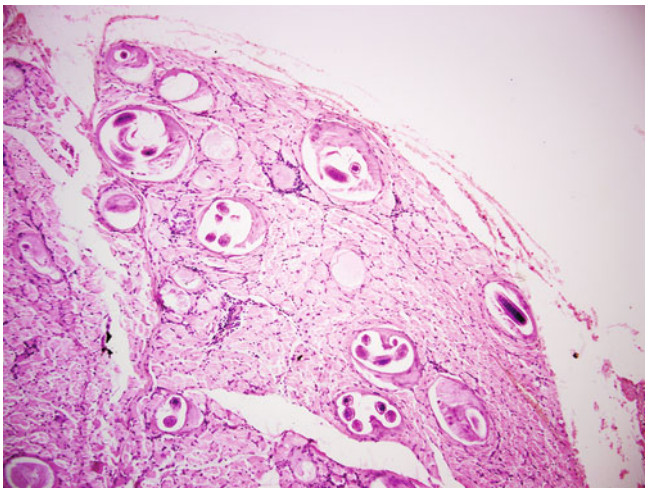

Fig. 5.62 Trichinosis is caused by nematodes of the species *Trichinella spiralis*. Sometimes referred to as the "pork worm," the infective form of the worm is also notably found in a variety of other animals, including bears and horses. Humans become infected by ingesting undercooked meat containing encysted larvae from these animals. When adult forms mature in the small intestinal mucosa, they release larvae that migrate to striated muscle, where they encyst. The cyst resides within a striated muscle cell often referred to as a "nurse cell." Several nurse cells containing encysted larval forms of *T. spirallis* are shown. Note the surrounding striated, skeletal muscle tissue. H&E, 100× magnification

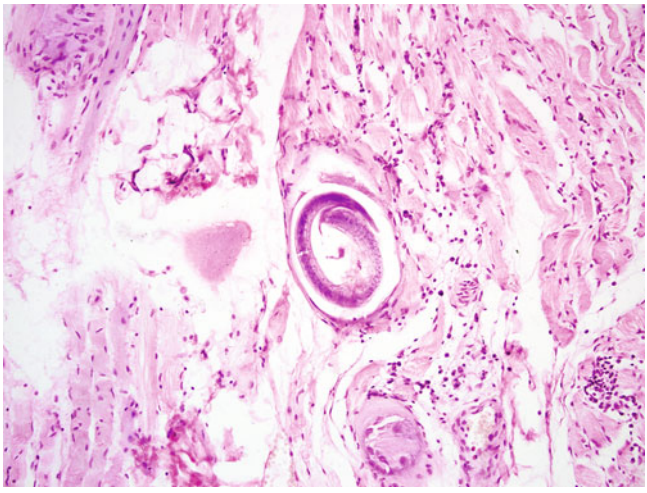

Fig. 5.63 Coiled *T. spiralis* larva within a nurse cell. H&E, 200× magnification

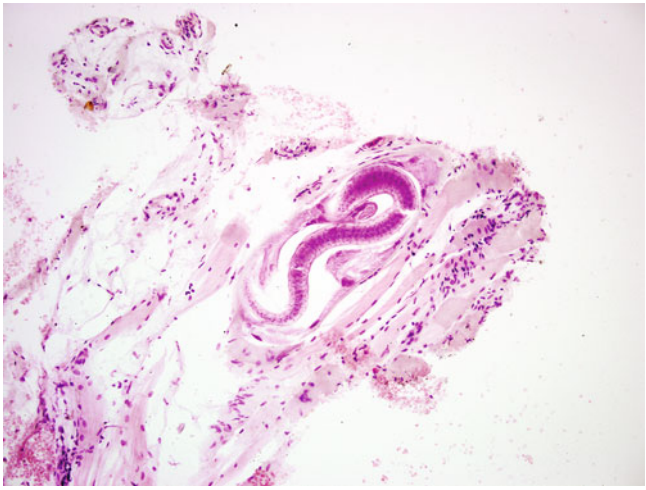

Fig. 5.64 While a tightly coiled larval form is the classic appearance of this parasite, this image demonstrates a larval form in a more relaxed state. H&E, 200× magnification

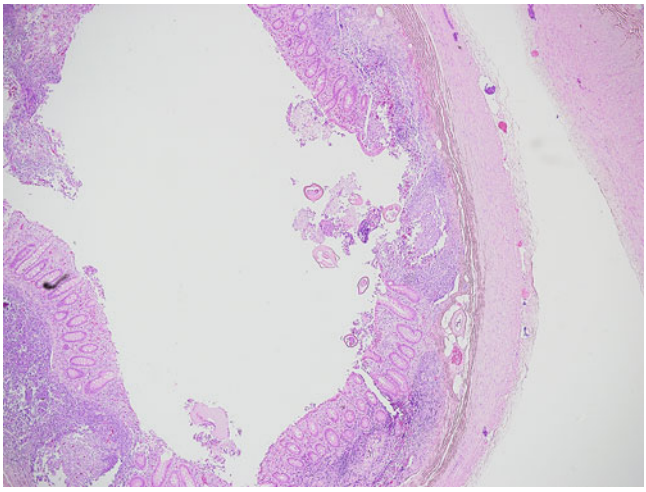

Fig. 5.65 *Enterobius vermicularis*, commonly referred to as "pinworm," is a common cause of pediatric perianal pruritus, worldwide. While most commonly identified by visualization of the eggs by the "scotch tape" method or variations thereof, the worms are occasionally seen in appendectomy specimens. In this location, they are usually considered an incidental finding but have rarely been implicated as a cause of appendicitis. Vermiform appendix demonstrating cross-sections of *E. vermicularis*. H&E, 40× magnification

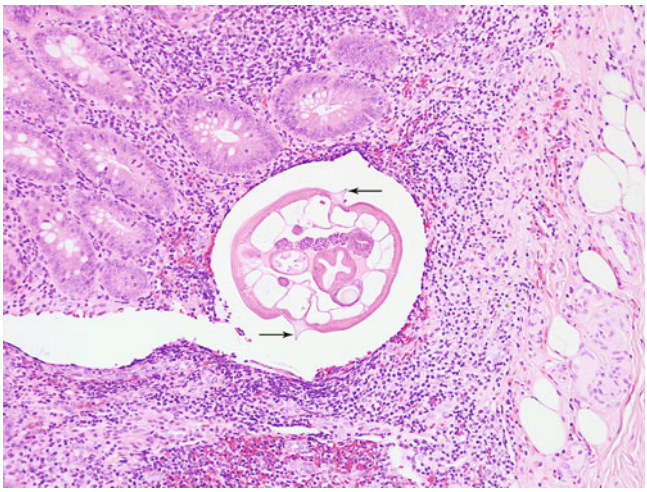

Fig. 5.66 Higher magnification image demonstrating prominent lateral alae (*arrows*). Note that a few more infrequently encountered nematodes, such as *Baylisascaris* species, also have lateral alae; however, the location in the appendix strongly indicates *E. vermicularis*. H&E, 200× magnification

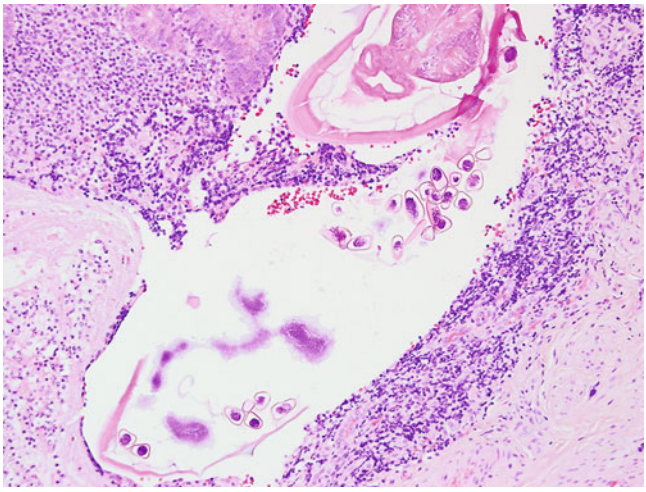

Fig. 5.67 Characteristic eggs of *E. vermicularis* which may be found inside the worms, or nearby, may also be helpful for identification. The eggs tend to be oval with a slightly flattened edge visible, depending on the plane of section. H&E, 200× magnification

Fig. 5.68 An egg of *E. vermicularis* obtained from a wet mount. Note that it is slightly flattened on one side. 400× magnification (Image courtesy of Dr. Ryan Relich)

5.2 Protozoal Infections

The protozoa are a diverse group of unicellular eukaryotic organisms. Covered here are the most commonly identified members within anatomic pathology. Many protozoa are more frequently identified in blood or in stool specimens. As these specimen types are not generally the focus of anatomic pathology, they are only discussed as relevant to an anatomic pathology practice here.

5.2.1 Malaria

Cerebral malaria is the most severe complication of infection with *Plasmodium falciparum*, the most common and virulent species, and can lead to encephalopathy, seizures, coma, and death. Survivors often experience long-term neural sequelae. High parasitemia as well as the ability of *P. falciparum* infected cells to sequester in terminal blood vessels can lead to microinfarction of a variety of different organs. Some studies suggest that host response to the infection may also play a role in end organ damage (Figs. 5.69, 5.70, 5.71 and 5.72).

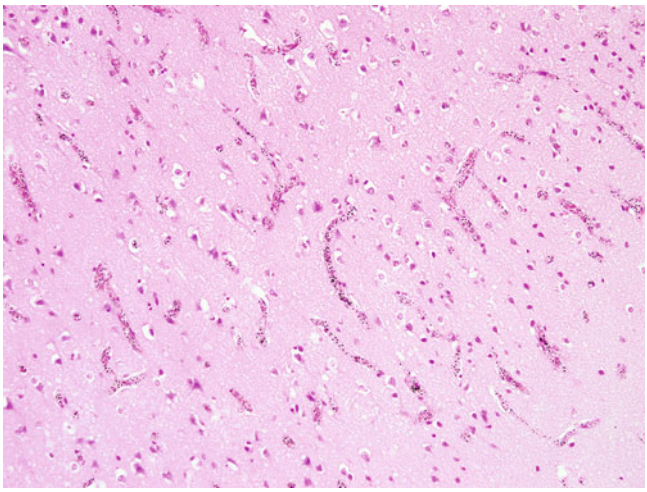

Fig. 5.69 Brain tissue demonstrating dilated blood vessels containing numerous red blood cells infected with late trophozoite stages of *P. falciparum*. Abundant dark malarial pigment is also characteristic. H&E, 200× magnification

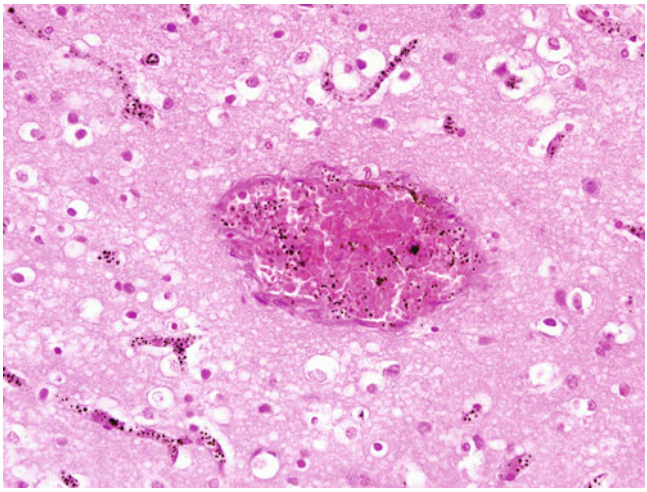

Fig. 5.70 Higher magnification image demonstrating congestion of a blood vessel in a case of cerebral malaria with abundant dark malarial pigment. H&E, 400× magnification

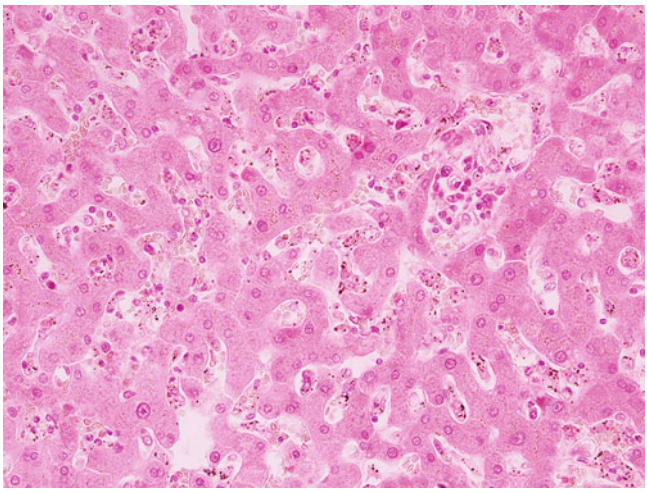

Fig. 5.71 Numerous parasitized and uninfected red blood cells within the sinusoids of the liver in a severe case of *P. falciparum* infection. Note expansion of the sinusoids and abundant malarial pigment. H&E, 400× magnification

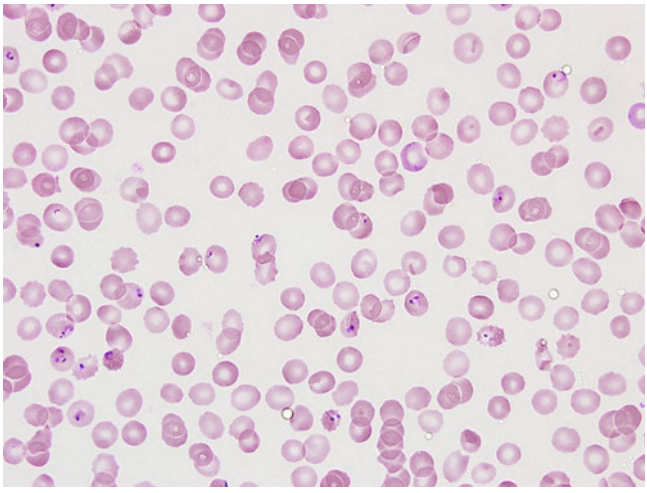

Fig. 5.72 Blood smear remains the mainstay of diagnosis for malaria. If histopathology is suggestive of organ infection with *Plasmodium*, blood smears or other diagnostic methods should be performed as part of the diagnostic workup. The infected red blood cells of the majority of *P. falciparum* infections, as seen here, demonstrate early trophozoite "ring" forms only, a feature that may be helpful for diagnosis. Rarely, banana-shaped gametocytes may also be seen. Giemsa stain, 1000× magnification

5.2.2 Toxoplasmosis

In human infections with *Toxoplasma gondii,* the organism will form cysts in a variety of organs, including the brain, skeletal muscle, heart, and eyes. The cysts contain the slowly reproducing, bradyzoite form of the parasite and persist for life, often being only an incidental finding at autopsy in patients who are not immunocompromised. Primary infection with or a reactivation of *T. gondii* infection in an immunocompromised host may be life threatening (Figs. 5.73, 5.74, 5.75 and 5.76).

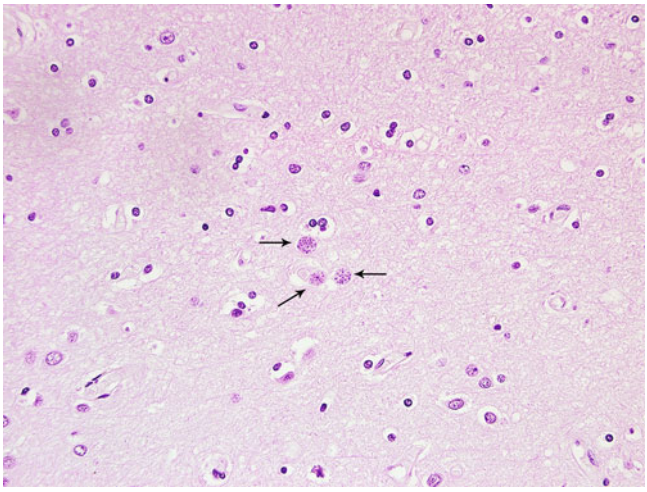

Fig. 5.73 Cysts containing bradyzoite forms of *T. gondii* in cerebral tissue (*arrows*). H&E, 400× magnification

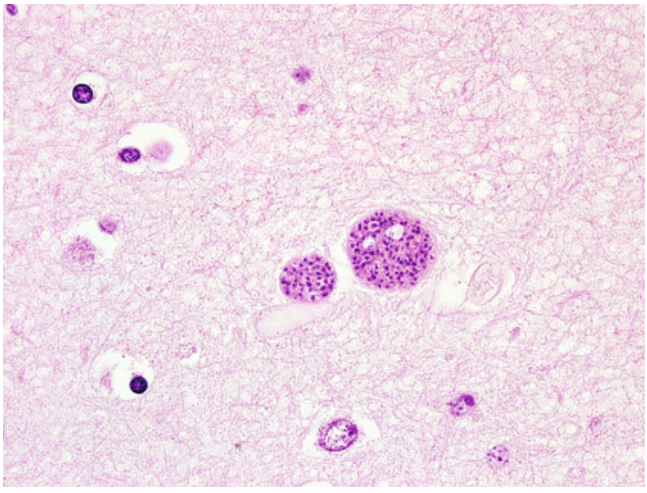

Fig. 5.74 Higher magnification image of *T. gondii* cysts in the brain containing numerous bradyzoite forms. H&E, 1000× magnification

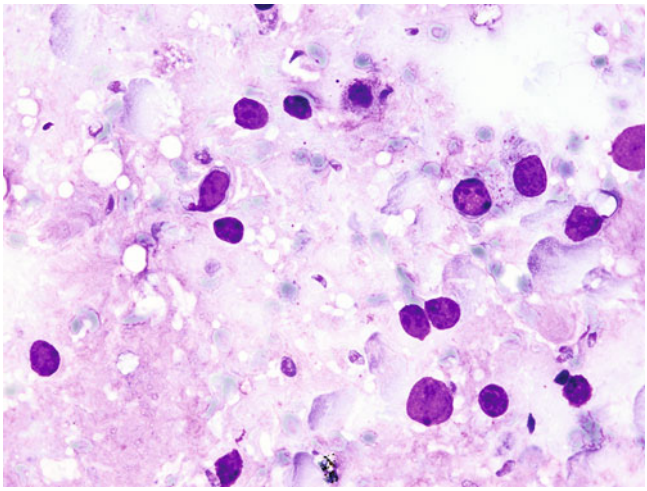

Fig. 5.75 The tachyzoite or rapidly reproducing form of *T. gondii* is seen in active infections. It is characteristically crescent-shaped, but several oval shaped forms are seen here as well. Brain biopsy tissue smear. Giemsa stain, 1000× magnification

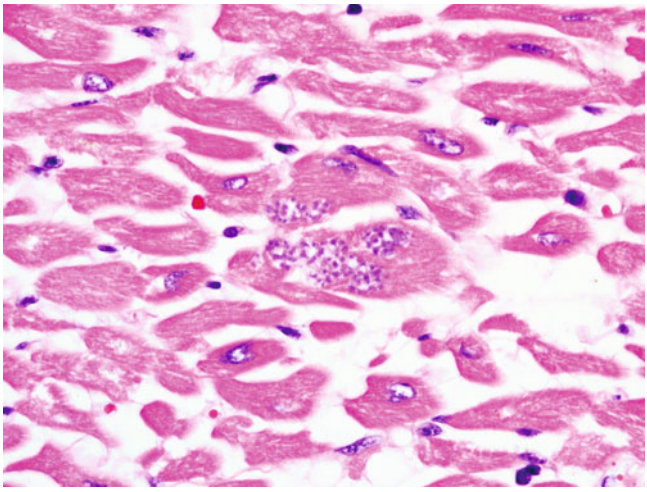

Fig. 5.76 Bradyzoites may be found in a wide variety of tissues. Seen here are cysts identified in cardiac muscle sampled during autopsy. H&E, 1000× magnification

5.2.3 Trypanosomiasis

Clusters of amastigote forms of *Trypanosoma cruzi* may appear microscopically similar to *Toxoplasma* cysts. They are more commonly found in cardiac muscle, which is a relatively rare location to find *Toxoplasma* species, the previous example not withstanding (Figs. 5.77 and 5.78).

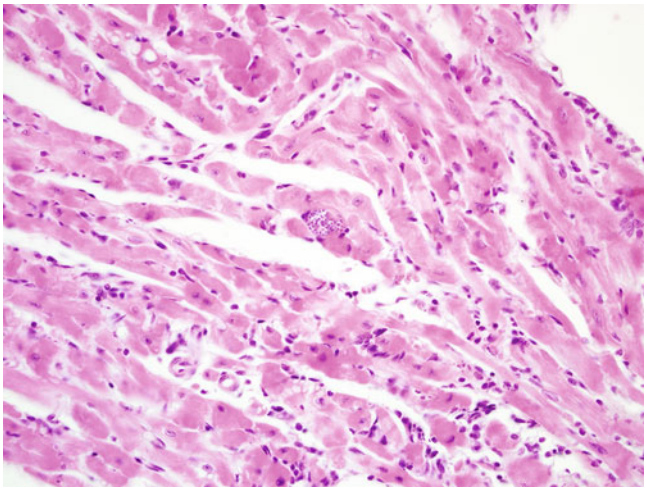

Fig. 5.77 *T. cruzi* amastigotes tend to cluster in looser aggregates, unlike the generally round, packed bradyzoite cyst forms of *Toxoplasma* species. H&E, 400× magnification

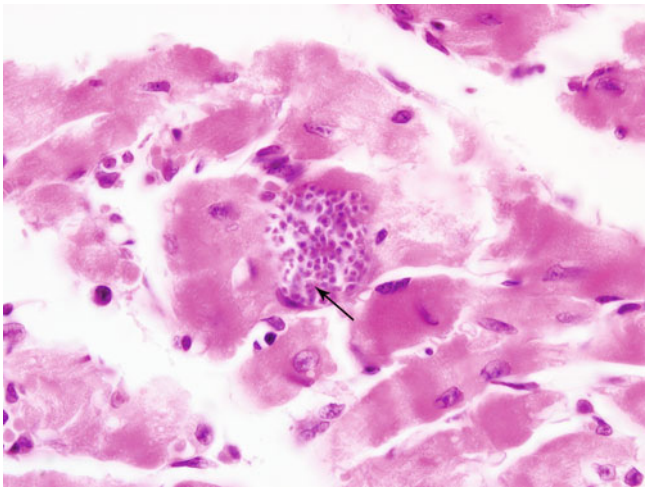

Fig. 5.78 At higher magnification, the loose aggregation of *T. cruzi* is more apparent. The organisms have a single nucleus and a bar shaped kinetoplast, which bradyzoites of *Toxoplasma* lack. The kinetoplast (*arrow*) is often very difficult to visualize on tissue sections. H&E, 1000× magnification

5.2.4 Leishmaniasis

Infection with *Leishmania* species can have several different forms, including cutaneous, mucocutaneous, and visceral leishmaniasis (kala-azar). The disease is endemic in areas where sandflies, the vector, are common. Cutaneous lesions manifest at the site of the initial bite, often appearing as a shallow, crater-like lesion, while visceral leishmaniasis manifests typically as fever accompanied by splenomegaly. Cutaneous manifestations may also occur following visceral leishmaniasis. Microscopically, the amastigotes of *Leishmania* species are indistinguishable from those of *T. cruzi*, a fact complicated by significant cross-reactivity of serologic assays, especially since they have overlapping endemicity in Central and South America. When organisms are found in the skin and bone marrow especially, the yeast forms of *Histoplasma capsulatum* may also enter the differential diagnosis. This is particularly important because both of these entities are commonly found in an intracellular location. Identification of the bar-shaped kinetoplast in *Leishmania* species can be helpful in determining a correct identification. Use of a Gomori methenamine silver stain may also be a useful method of ruling out *Histoplasma* since the yeast cells should stain black, while *Leishmania* do not stain (Figs. 5.79, 5.80, 5.81 and 5.82).

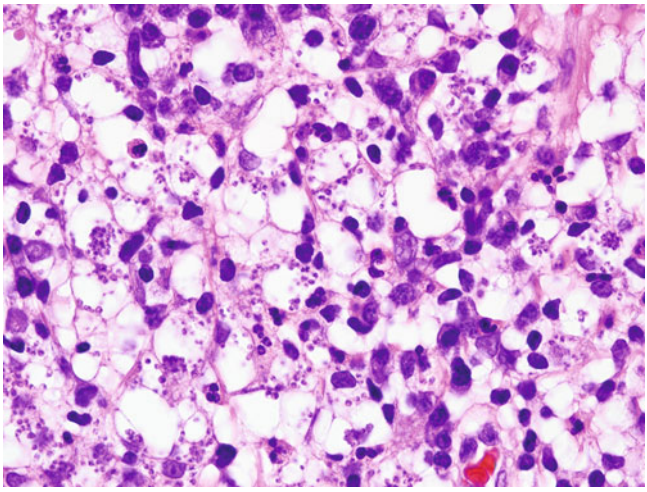

Fig. 5.79 Cutaneous lesion of leishmaniasis demonstrating many amastigotes within vacuolated appearing tissue. H&E, 500× magnification

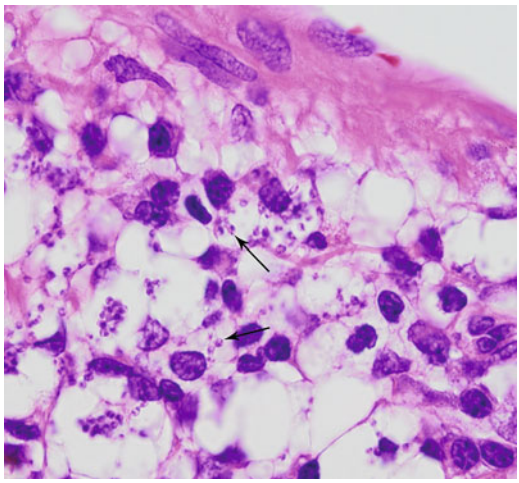

Fig. 5.80 At higher magnification, bar-shaped kinetoplasts can be identified in several of the amastigotes. H&E, 1000× magnification

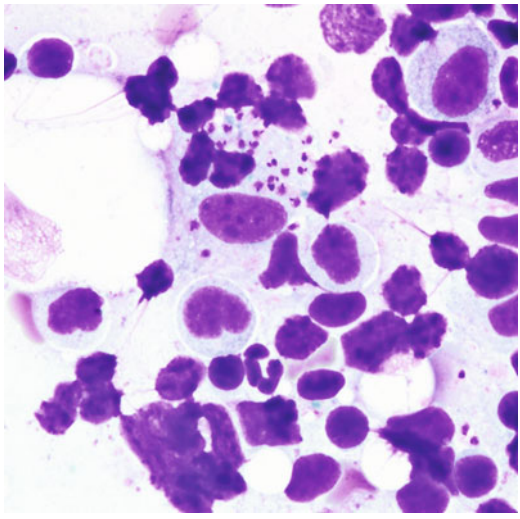

Fig. 5.81 Bone marrow aspirate remains the gold standard for the diagnosis of kala-azar. In some cases, splenic aspirates are performed, but this procedure is generally to be avoided if a bone marrow aspirate can be obtained, since it may carry significant risk to the patient. These methods also provide specimens for culture and further speciation of the organism by molecular methods. Bone marrow aspirate; note the presence of intracellular organisms. The kinetoplast is often much easier to visualize on cytologic/hematologic preparations. Diff-Quik stain, 1000× magnification

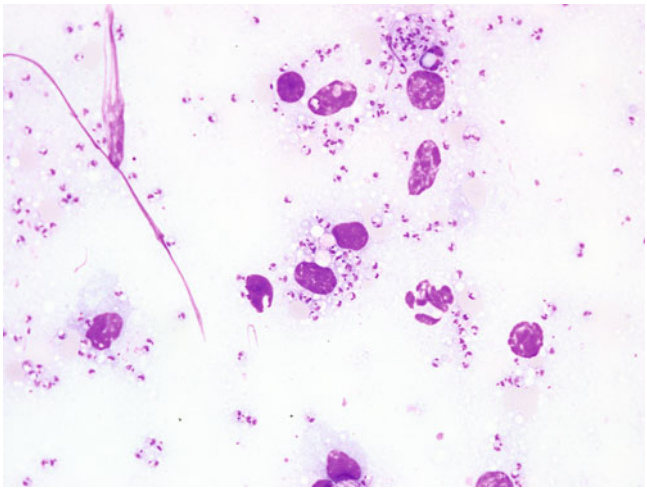

Fig. 5.82 Splenic aspirate. Again note the presence of intra- and extracellular organisms. Bar shaped kinetoplasts are clearly visible on this preparation. Giemsa stain, 1000× magnification

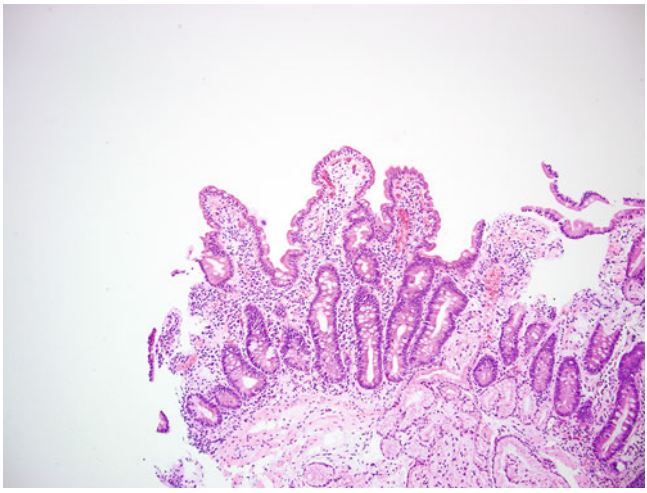

Fig. 5.83 Small intestine demonstrating villous blunting and a moderately increased inflammatory infiltrate in a case of cryptosporidiosis. H&E, 100× magnification

5.2.5 Cryptosporidiosis

This organism is a common but under-recognized cause of diarrhea, mostly within the pediatric population. Infection is through the fecal-oral route, by ingestion of the hardy oocyst form. While the organism can be identified by microscopic examination of stool, where the oocysts stain with modified acid-fast stains, and by direct fluorescent antibody stains, enzyme immunoassay (EIA) methods, or polymerase chain reaction (PCR) can also be used. The organism is also occasionally identified in gastrointestinal biopsy tissue (Figs. 5.83, 5.84 and 5.85).

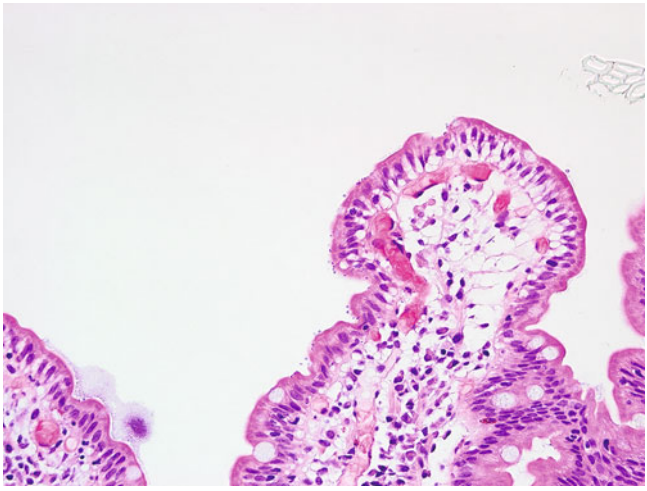

Fig. 5.84 On higher magnification, small (2–5 micron) basophilic, "blue bodies" are seen at the luminal surface. H&E, 400× magnification

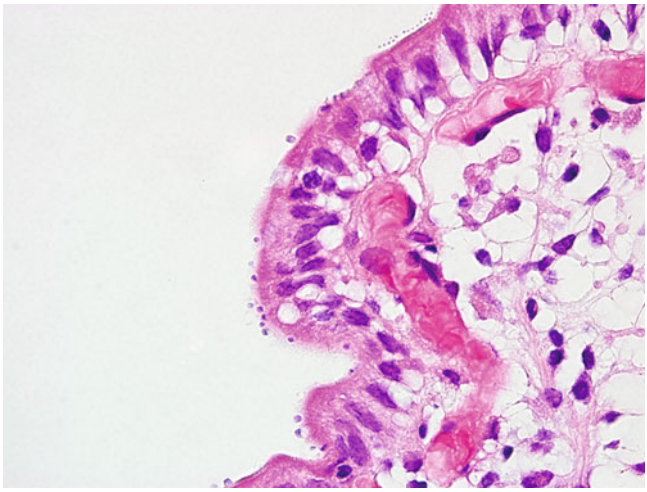

Fig. 5.85 Further magnification image demonstrating blue bodies at the luminal surface. While light microscopic examination suggests that the organisms are resting on the brush border of the small intestinal villi, they are in fact covered by a thin membrane and are intracellular. H&E, 1000× magnification

5.2.6 Giardiasis

Infection with *Giardia duodenalis* (syn. *G. lamblia, G. intestinalis*) typically demonstrates no to minimal villous blunting with minimal increase in inflammatory infiltrates. Diarrheal illness caused by infection with this organism is caused by malabsorption rather than toxin secretion or intestinal invasion. Also a common cause of parasitic diarrhea in the Western world (and indeed worldwide), *Giardia* is spread by ingestion of the cyst form of the organism (Figs. 5.86, 5.87 and 5.88).

Fig. 5.86 Small intestine; note the minimal to absent villous blunting with no increase in typical inflammatory cell composition. H&E, 100× magnification

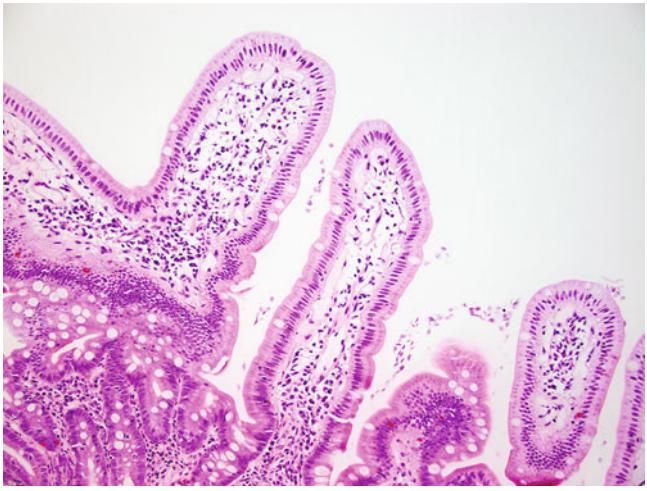

Fig. 5.87 At higher magnification, the organisms are more apparent and appear between the small intestinal villi. At first glace they may appear to be cellular debris. Importantly, they frequently do not appear in histopathologic section as the classic teardrop-shaped organisms with two prominent nuclei but are instead sectioned in multiple planes. H&E, 200× magnification

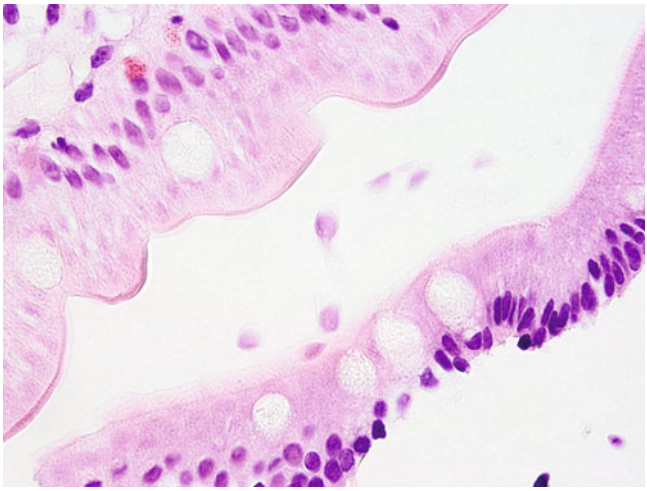

Fig. 5.88 Classic teardrop-shaped *Giardia* trophozoite. Note that on H&E staining, the two nuclei that make up the eyes of the "clown face" that *Giardia* is known for often stain very faintly. The organism also has four pairs of flagella that are usually difficult to appreciate on H&E staining, but they can sometimes be seen on other preparations such as trichrome or Giemsa. H&E, 1000× magnification

5.2.7 Amebic Infections

Amebic infections include amoebic colitis, soft tissue, and solid organ infections (most commonly liver) and are caused primarily by *Entamoeba histolytica*. Granulomatous amoebic encephalitis, caused by *Balamuthia mandrillaris* or by *Acanthamoeba* species, is characterized by a protracted course often lasting weeks to months, whereas primary amoebic meningoencephalitis caused by infection with *Naegleria fowleri* is typically fatal within approximately 5 days following onset of symptoms. *Acanthamoeba* species are also known to be causes of amoebic keratitis as well as subcutaneous soft-tissue infections (Figs. 5.89, 5.90, 5.91, 5.92, 5.93, 5.94, 5.95, 5.96 and 5.97).

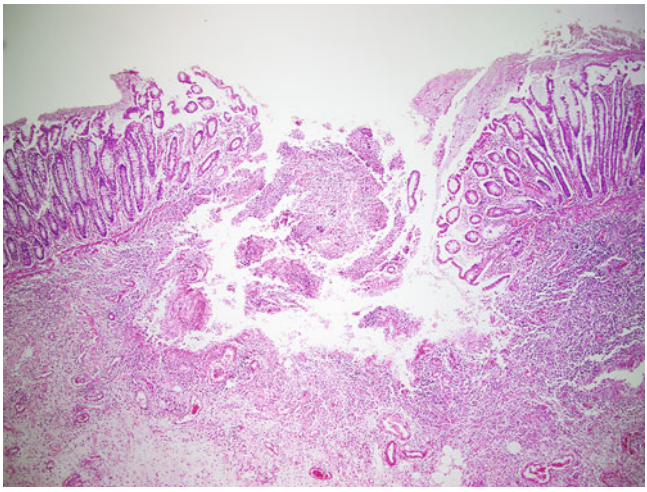

Fig. 5.89 Amebic colitis due to infection with *E. histolytica* classically demonstrates a "flask" shaped lesion with a relatively narrow opening through the mucosal surface and a widened base as the organisms progress deeper into the tissue. H&E, 40× magnification

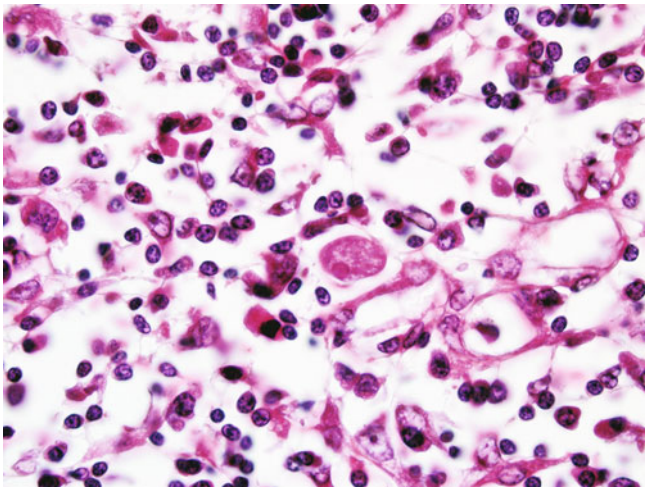

Fig. 5.90 *E. histolytica* trophozoites within colon tissue. The amoeba somewhat resembles a macrophage but has a well-circumscribed, round nucleus, with a centrally located, pinpoint karyosome. The karysome may be difficult to identify on H&E staining. The organisms are often easier to find at the edges of the lesion. H&E, 1000× magnification

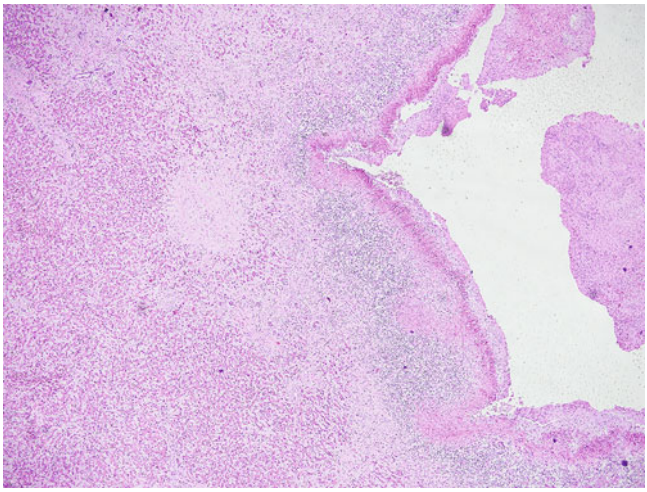

Fig. 5.91 Amoebic liver abscess caused by infection with *E. histolytica*. Grossly, these lesions may be filled with a reddish-brown fluid, often referred to as "anchovy paste." Aspiration of a suspected amoebic abscess for diagnostic purposes is generally not recommended. There is some risk that the abscess may leak post procedure resulting in amoebic peritonitis or that the needle tract may become seeded with organisms, worsening the problem. Additionally, organisms tend to congregate at the edge of lesions and are not likely to be properly sampled by a fine needle aspirate. Serologic testing in conjunction with radiologic findings is therefore the diagnostic method of choice. Most do not need to be removed surgically, but instead can be treated with amoebicidal drugs. Therapeutic aspiration is an option for large abscesses and may yield material for cytology, but organisms can be difficult to identify for the reasons stated above. Microscopically, resected lesions tend to have a "ragged" appearance, with more abundant organisms located at the edge. H&E, 40× magnification

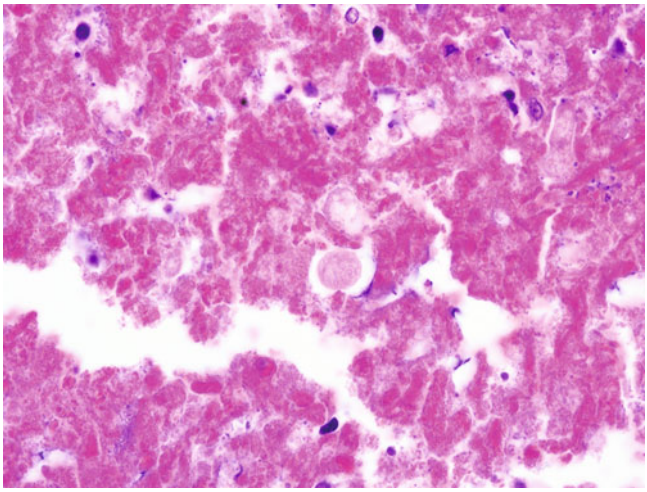

Fig. 5.92 *E. histolytica* trophozoite forms may be found within the necrotic tissue and at the edge of the lesion. In this particular example, the nucleus is only poorly visualized. H&E, 1000× magnification

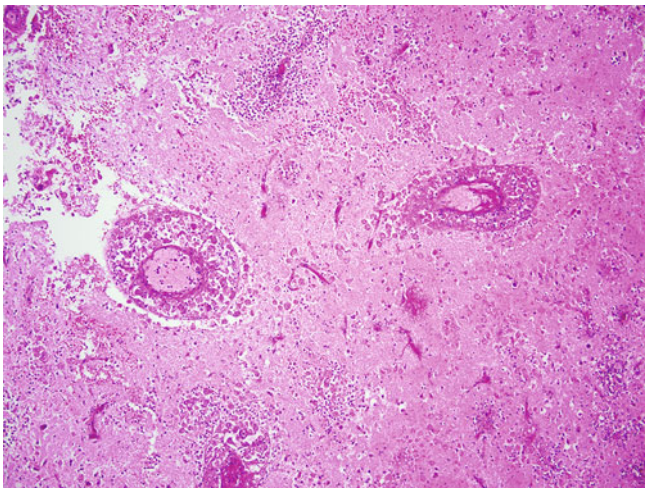

Fig. 5.93 Meningoencephalitis in a case of granulomatous amebic encephalitis (GAE). This entity is caused by either *Balamuthia mandrillaris* or *Acanthamoeba* species. As there is significant overlap in morphologic features between the two, differentiation by microscopy alone is not reliable. The causative agent in this case was later identified as *B. mandrillaris* by molecular identification methods. While presentations vary, a mixture of acute and granulomatous inflammation is typically seen. Note also the presence of many amoebae within the walls of the blood vessels. H&E, 200× magnification

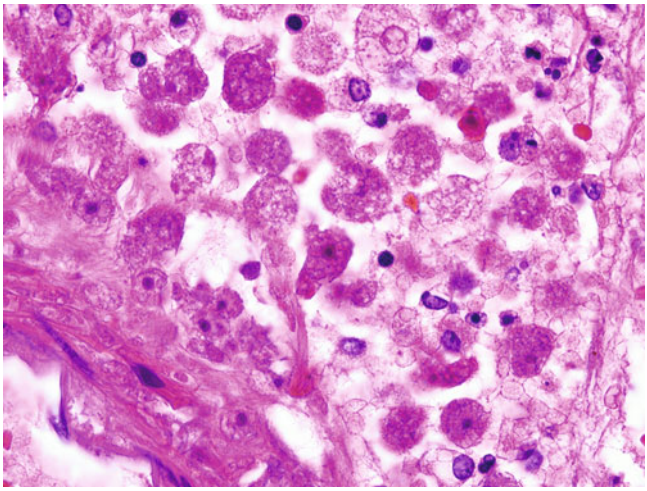

Fig. 5.94 At higher magnification, many trophozoite forms are evident within a blood vessel wall. Note that several of these organisms feature a prominent, large karyosome, a feature that is common in the free living amoebae, unlike the pinpoint karysome of *E. histolytica*. H&E, 1000× magnification

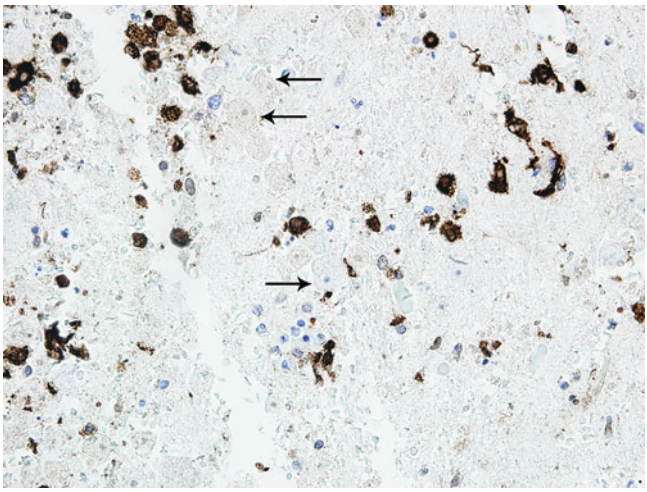

Fig. 5.95 The amoebae can be intermingled with macrophages, which being of the same approximate size and having a similar morphology, may present an additional diagnostic challenge. Immunohistochemical staining with CD68, which is expressed by monocytes and macrophages but not by amoebae, may be helpful in these cases. Note positive staining macrophages but also large nonstaining amoebae in the background (examples at *arrows*). CD68, 400× magnification

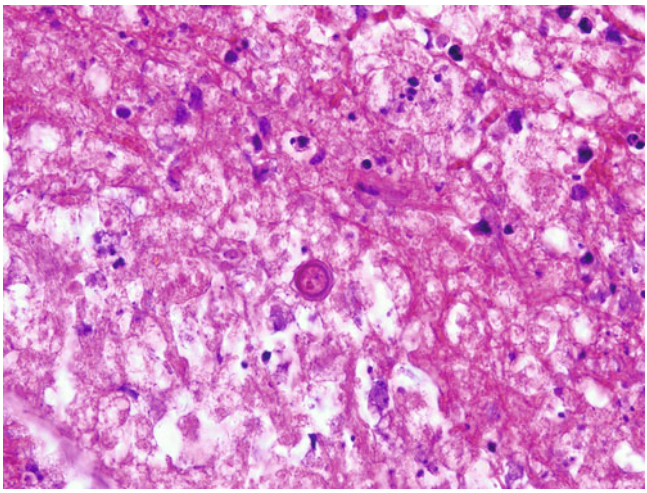

Fig. 5.96 Cyst forms of *B. mandrillaris* or *Acanthameoba* species are often seen in cases of GAE. The causative agent of primary amebic meningoencephalitis (PAM), *Naegleria fowleri,* does not produce cyst forms in human tissue. The clinical course of PAM is also notably more acute, differentiating it from GAE. H&E, 1000× magnification

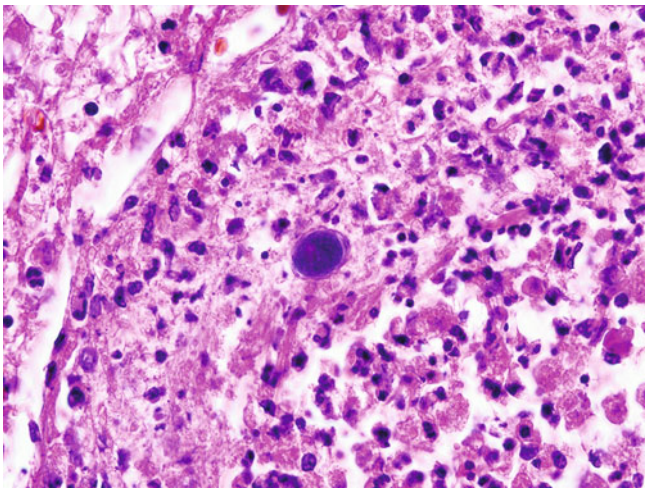

Fig. 5.97 Another example of a cyst form from the previously discussed case. The staining of the inner cyst (endocyst) with H&E can vary, appearing more basophilic in this example. Also note the characteristic "wrinkled" appearance of the outer wall (the exocyst). H&E, 1000× magnification

5.3 Ectoparasites

Ectoparasites, by definition, live on but not inside the body. From an anatomic pathology perspective the most frequently encountered of these will be arthropod adult or larval forms living within cutaneous or subcutaneous tissue. While most of the ectoparasites discussed here are better identified by submission to the microbiology laboratory, they are occasionally encountered within surgical specimens as incidental findings or because of initial misidentification. Ticks in particular may present grossly in many different ways, depending on stages of engorgement from a blood meal; they often appear as moles, seborrheic keratoses, or infarcted skin tags. While the ectoparasites of humans are extensive, this section concentrates on those that may most frequently wind up under the lens of the anatomic pathologist (Figs. 5.98, 5.99, 5.100, 5.101, 5.102, 5.103, 5.104, 5.105, 5.106, 5.107, 5.108 and 5.109).

Fig. 5.98 Hard ticks, such as *Dermacentor variabilis* pictured here, have a hard exoskeleton containing chitin. These ticks additionally exhibit a backplate called a scutum, which in Latin means "shield." Males have a scutum that extends over their entire backs, while females feature a scutum that extends only approximately 1/3 of the way down the back. The shorter scutum allows for females, which take much larger blood meals, to expand. As females tend to feed for much longer, often several days, they are the more likely of the two sexes to be biopsied or otherwise removed and submitted to surgical pathology. Soft ticks, as the name suggests, have a membranous outer surface and are more frequently parasites of animals, seldom encountered in human anatomic pathology. In male *D. variabilis* (*left*), note the ornate scutum which extends fully over the back. In a partially engorged female *D. variabilis* (*right*), note the smaller scutum and the significant overall increase in size and deformity in shape, leading to misidentification as a variety of cutaneous growths. A fragment of skin remains attached to the mouthparts

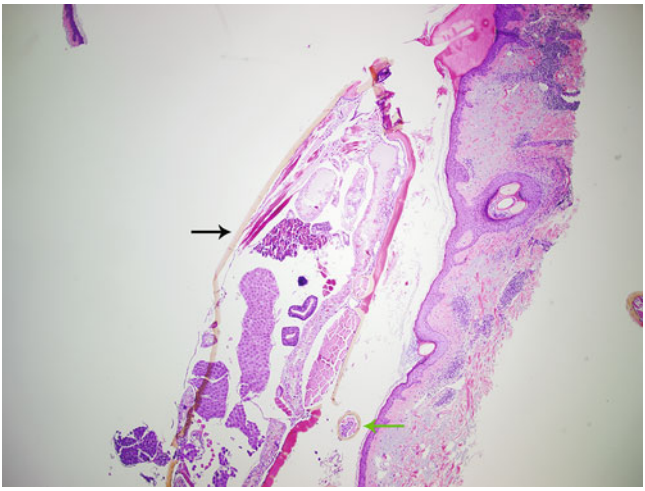

Fig. 5.99 Skin biopsy demonstrating sections through a hard tick. Note that speciation at this point is nearly impossible. If recognized as a tick, submission to microbiology of the whole arthropod, or its remaining parts for identification is preferable, as the species will dictate which diseases it may possibly transmit to the human host. A chitinous scutum is evident and appears yellow on H&E staining (*black arrow*). A thick, eosinophilic cuticle is seen as well. Internally, muscle fibers and various organ structures are noted. A cross-section of a leg demonstrating skeletal muscle is also seen (*green arrow*). H&E, 40× magnification

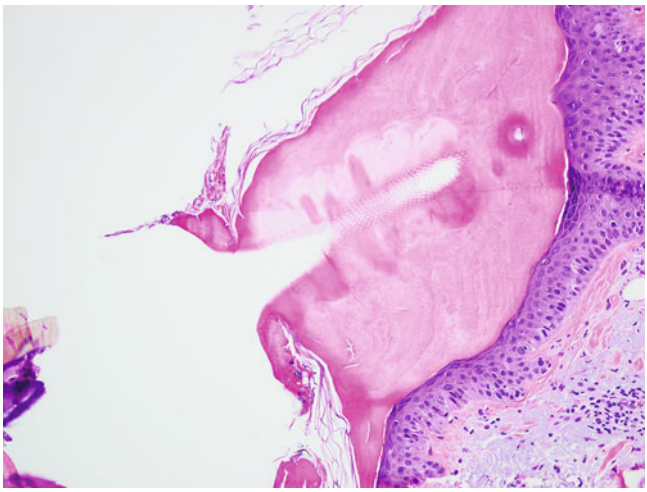

Fig. 5.100 Ticks feed by means of a hypostome, often described as a needle-like structure which penetrates the skin allowing access to the hosts blood. The hypostome of most ticks features recurved barbs that serve to further anchor the tick in place during feeding. Its hold is so strong that it, along with other mouthparts and the head of the tick, is often retained in the host after removal is attempted. Shown here is a fortuitous section demonstrating an embedded hypostome with prominent barbs. H&E, 200× magnification

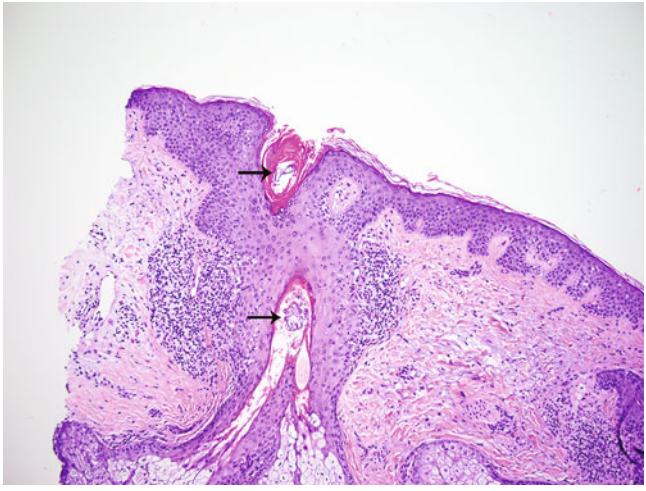

Fig. 5.101 *Demodex* mites are very common findings in skin biopsy sections and are usually considered to be commensal organisms of cutaneous pilosebaceous structures. They have, however, been implicated as a cause of folliculitis, blepharitis, and rosacea among other conditions. *Demodex* has an elongate appearance with a head, a thorax that contains four pairs of rudimentary legs, and a long, tail-like abdomen. While it is generally not important to differentiate between the two primary species that infect humans, *D. folliculorum* tends to reside within hair follicles, and the shorter *D. brevis* usually inhabits the sebaceous glands. Note fragments of mite parts within the hair shaft (*arrows*) in a case of perifolliculitis associated with *D. folliculorum*. H&E, 100× magnification

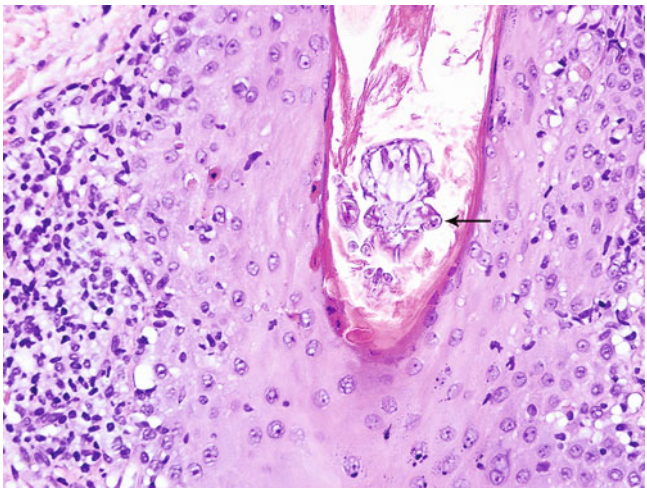

Fig. 5.102 Higher magnification image demonstrating the head and thorax of *D. folliculorum*. The arrow highlights an example of the rudimentary legs extending from the thorax that can sometimes be seen. H&E, 400× magnification

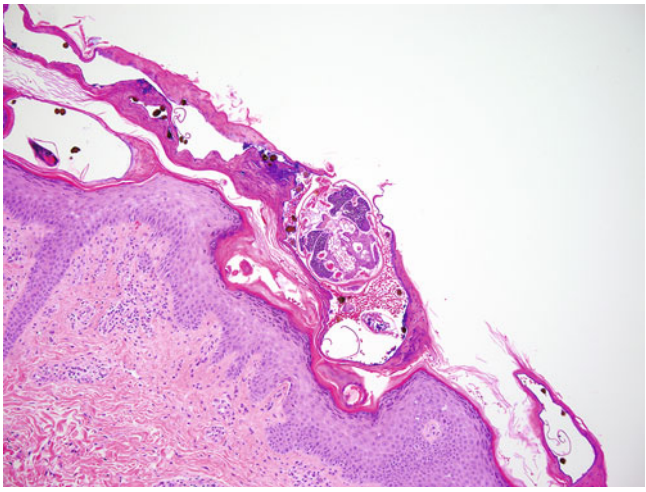

Fig. 5.103 Infestations by *Sarcoptes scabiei* can be found in a variety of cutaneous locations, with a predilection for the finger webs, wrists, axillae, and genital regions. The rash caused by scabies is usually very pruritic and may also result in the formation of papules or pustules. On biopsy, arthropod parts, eggs, and scybala, the yellowish-brown fecal pellets seen in this image, may be noted in the subcorneal region. The inflammatory response immediately surrounding the mites tends to be neutrophilic with a lymphocytic and eosinophilic component within the underlying dermis. H&E, 100× magnification

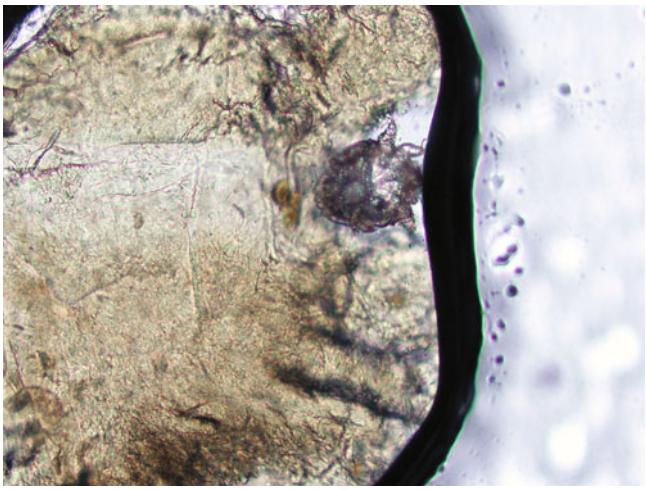

Fig. 5.104 Seen here is a whole *Sarcoptes scabiei* mite obtained from skin scrapings and placed onto a slide with a few drops of mineral oil, the preferred collection method for identifying scabies in the microbiology laboratory. A second slide can then be placed on top, sealing the specimens inside for later observation under the microscope. 100× magnification (Image courtesy of Jeremy Koehlinger)

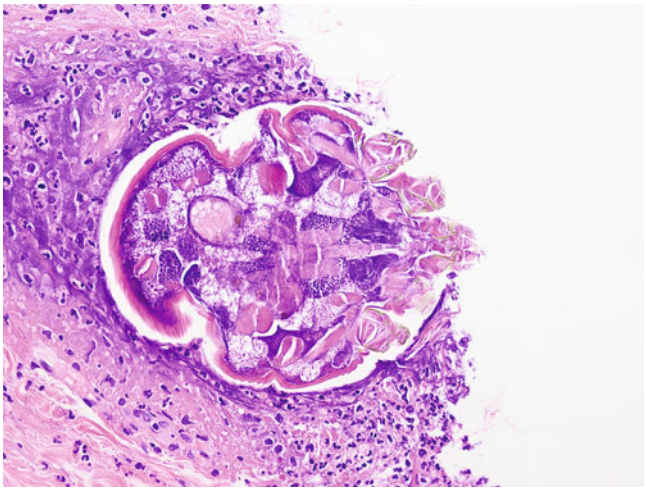

Fig. 5.105 A near perfect coronal section through a *S. scabiei* mite. Compare to Fig. 5.104. H&E, 400× magnification

Fig. 5.106 Larva of *Dermatobia hominis*, more commonly known as the human botfly. Full grown larvae measure between 15 and 20 mm in length. Note the rows of dark cuticular spines which ring the body. Other causes of myiasis, such as *Cordylobia anthropophaga,* more commonly known as the tumbu fly, can have a similar gross appearance, although the spines tend to be more randomly distributed. As such, evaluation by a parasitologist or thorough examination utilizing one of many excellent medical parasitology atlases may be required for definitive identification. A history of travel to certain parts of the world (botflies are found in Mexico as well as Central and South America, while tumbu flies are found in tropical Africa) may also be helpful. Specimens that are surgically resected are found in a subdermal cavity, where the larva feeds on surrounding tissues

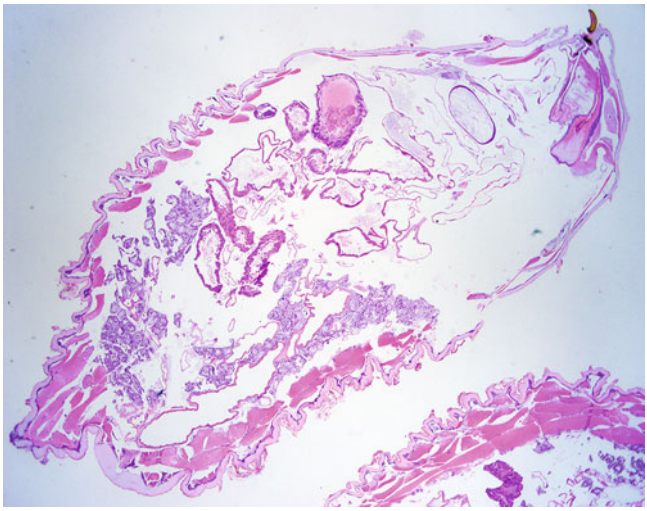

Fig. 5.107 Sections of *D. hominis* larvae that were submitted for surgical pathology. Note the presence of many triangular cuticular spines as well as internal muscle fibers and various organ structures. A refractile, yellow-appearing portion of the curved mandibles of the larvae is also seen in the upper right portion of the section. H&E, 20× magnification

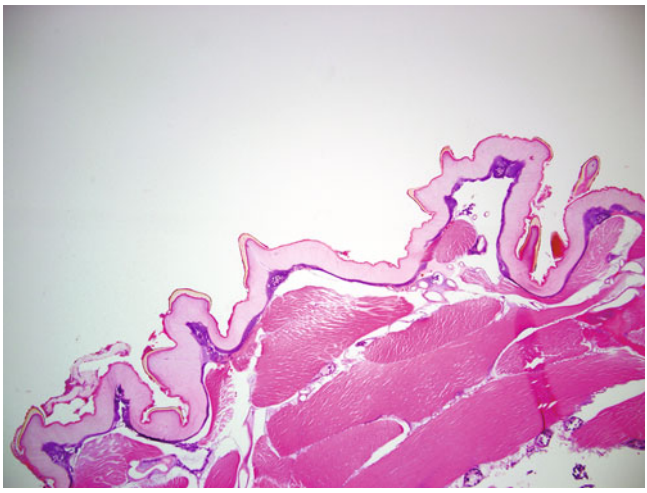

Fig. 5.108 Higher magnification image demonstrating sections through the cuticular spines. The spines appear yellow and refractile on H&E staining, having a vaguely triangular appearance. Note also bands of muscle fibers just below the cuticle. H&E, 100× magnification

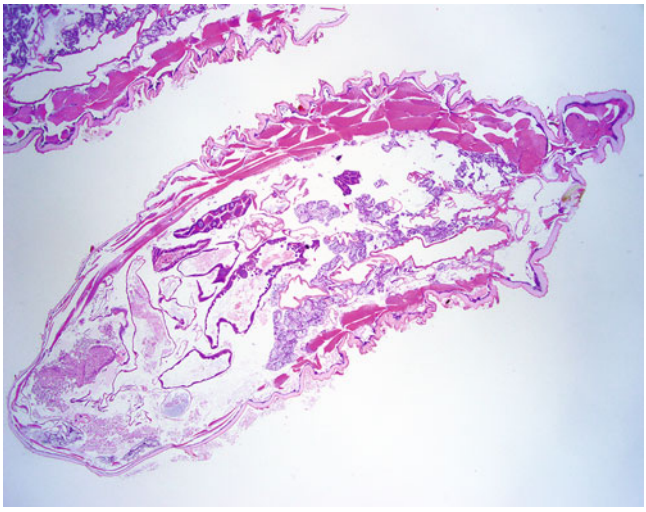

Fig. 5.109 Sections of *C. anthropophaga* larva determined by travel history. Note the similarity in microscopic appearance to the botfly larvae discussed above. Definitive identification is very difficult by histopathology alone and is best accomplished by gross examination of the larvae by an experienced parasitologist and correlation with the patient's travel history. H&E, 20× magnification

Suggested Reading

Al-Salem W, Herricks JR, Hotez PJ. A review of visceral leishmaniasis during the conflict in South Sudan and the consequences for East African countries. Parasit Vectors. 2016;9:460.

Angheben A, Boix L, Buonfrate D, Gobbi F, Bisoffi Z, Pupella S, et al. Chagas disease and transfusion medicine: a perspective from non-endemic countries. Blood Transfus. 2015;13:540–50.

Belizario Jr V, Delos Trinos JP, Garcia NB, Reyes M. Cutaneous manifestations of selected parasitic infections in Western Pacific and Southeast Asian regions. Curr Infect Dis Rep. 2016;18:30.

Bowen LN, Smith B, Reich D, Quezado M, Nath A. HIV-associated opportunistic CNS infections: pathophysiology, diagnosis and treatment. Nat Rev Neurol. 2016;12:662–74.

Cama VA, Mathison BA. Infections by intestinal Coccidia and Giardia duodenalis. Clin Lab Med. 2015;35:423–44.

Del Brutto OH, García HH. Taenia solium cysticercosis—the lessons of history. J Neurol Sci. 2015;359:392–5.

DuPont HL. Persistent diarrhea: a clinical review. JAMA. 2016;315:2712–23.

Faccini-Martínez ÁA, Pérez-Díaz CE, Botero-García CA, Benítez-Baracaldo FC, Rodríguez-López AE, Rodríguez-Morales AJ. Role of the blood smear in febrile returning travelers: beyond malaria. Travel Med Infect Dis. 2016;14:515–6.

Feldman DM, Keller R, Borgida AF. Toxoplasmosis, parvovirus, and cytomegalovirus in pregnancy. Clin Lab Med. 2016;36:407–19.

Gajurel K, Dhakal R, Deresinski S. Leishmaniasis in solid organ and hematopoietic stem cell transplant recipients. Clin Transplant. 2016; doi:10.1111/ctr.12867. [Epub ahead of print.]

Gonzales I, Rivera JT. Garcia HH; cysticercosis working group in Peru. Pathogenesis of Taenia solium taeniasis and cysticercosis. Parasite Immunol. 2016;38:136–46.

Guarner J, Bartlett J, Shieh WJ, Paddock CD, Visvesvara GS, Zaki SR. Histopathologic spectrum and immunohistochemical diagnosis of amebic meningoencephalitis. Mod Pathol. 2007;20:1230–7.

Kaplan KJ, Goodman ZD, Ishak KG. Eosinophilic granuloma of the liver: a characteristic lesion with relationship to visceral larva migrans. Am J Surg Pathol. 2001;25:1316–21.

Lala S, Upadhyay V. Enterobius vermicularis and its role in paediatric appendicitis: protection or predisposition? ANZ J Surg. 2016;86:717–9.

Lamps LW. Infectious causes of appendicitis. Infect Dis Clin N Am. 2010;24:995–1018.

Lobo SA, Patil K, Jain S, Marks S, Visvesvara GS, Tenner M, Braun A, Wang G, El Khoury MY. Diagnostic challenges in *Balamuthia mandrillaris* infections. Parasitol Res. 2013;112:4015–9.

Massolo A, Liccioli S, Budke C, Klein C. *Echinococcus multilocularis* in North America: the great unknown. Parasite. 2014;21:73.

O'Connell EM, Nutman TB. Molecular diagnostics for soil-transmitted helminths. AmJTrop Med Hyg. 2016;95:508–13.

Othman AA, Soliman RH. Schistosomiasis in Egypt: a never-ending story? Acta Trop. 2015;148:179–90.

Qian MB, Utzinger J, Keiser J, Zhou XN. Clonorchiasis. Lancet. 2016;387:800–10; doi:10.1099/jmmcr.0.005011.

Roiko MS, Schmitt BH, Relich RF, Meyer TL, Zhang S, Davis TE. An unusual presentation of leishmaniasis in a human immunodeficiency virus-positive individual. J Med Microbiol Case Rep. 2016; doi: 10.1099/jmmcr.0.005011. (ePub May 2, 2016).

Shimoni Z, Froom P. Uncertainties in diagnosis, treatment and prevention of trichinellosis. Expert Rev Anti-Infect Ther. 2015;13:1279–88.

Soares R, Tasca T. Giardiasis: an update review on sensitivity and specificity of methods for laboratorial diagnosis. J Microbiol Methods. 2016;129:98–102.

Starr MC, Montgomery SP. Soil-transmitted helminthiasis in the United States: a systematic review—1940–2010. Am J Trop Med Hyg. 2011;85:680–4.
Visvesvara GS. Amebic meningoencephalitides and keratitis: challenges in diagnosis and treatment. Curr Opin Infect Dis. 2010;23:590–4.
Wilhelm CL, Yarovinsky F. Apicomplexan infections in the gut. Parasite Immunol. 2014;36:409–20.
Yan C, Liang LJ, Zheng KY, Zhu XQ. Impact of environmental factors on the emergence, transmission and distribution of *Toxoplasma gondii*. Parasit Vectors. 2016;9:137.
Yoder JS, Eddy BA, Visvesvara GS, Capewell L, Beach MJ. The epidemiology of primary amoebic meningoencephalitis in the USA, 1962-2008. Epidemiol Infect. 2010;138:968–75.